Biochimica et Biophysica Acta 1852 (2015) 2170–2182

Contents lists available at ScienceDirect

Biochimica et Biophysica Acta

journal homepage: www.elsevier.com/locate/bbadis

Differential roles of MMP-9 in early and late stages of dystrophic muscles in a mouse model of Duchenne muscular dystrophy

Naoko Shiba [a], Daigo Miyazaki [b], Takahiro Yoshizawa [c], Kazuhiro Fukushima [d], Yuji Shiba [e], Yuji Inaba [a], Michihiro Imamura [f], Shin'ichi Takeda [f], Kenichi Koike [a], Akinori Nakamura [d,*]

[a] Department of Pediatrics, Shinshu University School of Medicine, 3-1-1 Asahi, Matsumoto 390-8621, Japan
[b] Department of Medicine (Neurology and Rheumatology), Shinshu University School of Medicine, 3-1-1 Asahi, Matsumoto 390-8621, Japan
[c] Division of Laboratory Animal Research, Research Center for Human and Environmental Sciences, Shinshu University, 3-1-1 Asahi, Matsumoto 390-8621, Japan
[d] Intractable Disease Care Center, Shinshu University Hospital, 3-1-1 Asahi, Matsumoto 390-8621, Japan
[e] Department of Cardiovascular Medicine, Shinshu University School of Medicine, 3-1-1 Asahi, Matsumoto 390-8621, Japan
[f] Department of Molecular Therapy, National Institute of Neuroscience, National Center of Neurology and Psychiatry, 4-1-1 Ogawahigashi, Kodaira 187-8561, Japan

ARTICLE INFO

Article history:
Received 30 March 2015
Received in revised form 5 July 2015
Accepted 8 July 2015
Available online 10 July 2015

Keywords:
Dystrophin
Fibrosis
MMP-9
MIP-2
MCP-1
Osteopontin

ABSTRACT

Matrix metalloprotease (MMP)-9 is an endopeptidase associated with the pathogenesis of Duchenne muscular dystrophy (DMD). The precise function of MMP-9 in DMD has not been elucidated to date. We investigated the effect of genetic ablation of MMP-9 in the *mdx* mouse model (*mdx*/*Mmp9*$^{-/-}$). At the early disease stage, the muscles of *mdx*/*Mmp9*$^{-/-}$ mice showed reduced necrosis and neutrophil invasion, accompanied by down-regulation of chemokine MIP-2. In addition, muscle regeneration was enhanced, which coincided with increased macrophage infiltration and upregulation of MCP-1, and resulted in increased muscle strength. The *mdx*/*Mmp9*$^{-/-}$ mice also displayed accelerated upregulation of osteopontin expression in skeletal muscle at the acute onset phase of dystrophy. However, at a later disease stage, the mice exhibited muscle growth impairment through altered expression of myogenic factors, and increased fibroadipose tissue. These results showed that MMP-9 might have multiple functions during disease progression. Therapy targeting MMP-9 may improve muscle pathology and function at the early disease stage, but continuous inhibition of this protein may result in the accumulation of fibroadipose tissues and reduced muscle strength at the late disease stage.

1. Introduction

Duchenne muscular dystrophy (DMD) is the most common muscular dystrophy and is a lethal, X-linked disorder that affects 1 in 3600 to 6000 male births [1]. The disease is caused by a mutation in the *DMD* gene encoding dystrophin, a 427 kDa cytoskeletal protein that is localized at the sub-sarcolemma and that is a major component of the dystrophin glycoprotein complex (DGC) which links the cytoskeleton to the extracellular matrix (ECM) [2–4]. Dystrophin deficiency results in the disruption of the DGC, leading to membrane fragility and subsequent muscle fiber necrosis with inflammation, and replacement of the skeletal muscle with adipofibrous tissues during chronic degeneration and regeneration cycles. The progressive dystrophic change is accelerated by the impairment of tissue repair and regeneration, along with muscle fiber deterioration; however, the underlying mechanism remains unclear.

Matrix metalloproteases (MMPs), a family of zinc-dependent endopeptidases, are important regulatory proteins in the formation, remodeling, and degradation of ECM components in both physiological processes such as bone morphogenesis and pathological processes such as tumor progression and metastasis, systemic vascular diseases, and rheumatoid arthritis [5,6]. The ECM is one of the key players in the homeostasis and maintenance of muscle fiber functional integrity in the skeletal muscle [7,8]. Furthermore, many non-matrix proteins such as chemokines, growth factors, and receptors have recently been revealed to be substrates for MMPs, indicating that MMPs may have a more complex role, especially in leukocyte recruitment during inflammation [9].

Abbreviations: β-DG, β-dystroglycan; CBB, Coomassie brilliant blue; CCR2, C–C motif chemokine receptor type 2; CK, creatine kinase; CNF, centronuclear fiber; CSA, cross-sectional area; CTX, cardiotoxin; $CXMD_J$, canine X-linked muscular dystrophy in Japan; DAB, diaminobenzidine; DAPI, 4′,6-diamidino-2-phenylindole; DGC, dystrophin glycoprotein complex; DMD, Duchenne muscular dystrophy; ECM, extracellular matrix; H&E, hematoxylin and eosin; IFN-γ, interferon-γ; IGF-1, insulin like growth factor-1; IgG, immunoglobulin G; IL, interleukin; MCP-1, monocyte chemotactic protein-1; MHC, myosin heavy chain; MIP-2, macrophage inflammatory protein-2; MMP, matrix metalloprotease; MPO, myeloperoxidase; nNOS, neuronal nitric oxide synthase; OPN, osteopontin; PBS, phosphate-buffered saline; PDGF, platelet-derived growth factor; PNF, perinuclear fiber; rRNA, ribosomal RNA; TA, tibialis anterior; SDS, sodium dodecyl sulfate; TGF-β, transforming growth factor-β; TIMP, tissue inhibitor of metalloproteinase; TNF-α, tumor necrosis factor-α; VEGFA, vascular endothelial growth factor-A; VEGFR, VEGF receptor; WT, wild-type

* Corresponding author.
E-mail address: anakamu@shinshu-u.ac.jp (A. Nakamura).

http://dx.doi.org/10.1016/j.bbadis.2015.07.008
0925-4439/

It has been reported that the activities of various MMPs were significantly elevated in dystrophic muscle of a dystrophin-deficient DMD mouse model *mdx* compared to wild-type (WT) mice [10]. In particular, MMP-2 (gelatinase A) and MMP-9 (gelatinase B) were shown to be upregulated in the skeletal muscles of *mdx* mice and of the canine X-linked muscular dystrophy in Japan ($CXMD_J$) model, predominantly in necrotic fibers invaded by inflammatory cells [11–13]. Furthermore, it has recently been reported that the level of MMP-9 is increased in serum and muscle biopsies from DMD patients and correlates with the disease progression [14]. Therefore, in addition to its role in ECM remodeling in normal skeletal muscle tissues, MMP-9 has been hypothesized to be involved in the DMD pathomechanism [11,15–17]. Recently, we have demonstrated that ablation of *MMP-2* in *mdx* mice resulted in the impairment of regenerated muscle fiber growth, which coincided with a decreased expression of vascular endothelial growth factor-A (VEGFA) and of neuronal nitric oxide synthase (nNOS), implying that MMP-2 is required for the growth of regenerated muscle fibers through angiogenesis in *mdx* skeletal muscle [18].

MMP-9 has been reported to cleave β-dystroglycan (β-DG), a core component of the DGC, resulting in the disruption of the link between the ECM and the cell membrane in dystrophin-deficient skeletal muscle [19,20]. Genetic ablation and pharmacological inhibition of MMP-9 in *mdx* mice were shown to reduce skeletal muscle inflammation and fibronecrosis, resulting in improved muscle function at the early disease stage [21,22], and to ameliorate cardiomyopathy and reduce fibrosis at a later disease stage (1-year-old *mdx* mice) [23]. Furthermore, it has recently been reported that the partial inhibition of MMP-9 caused a reduction in pro-inflammatory M1 macrophages and an increase in anti-inflammatory M2 macrophages, accompanied by an upregulation of Notch signaling, improving the muscle regeneration in young *mdx* mice [22]. However, little is known about the exact action of MMP-9 in dystrophic muscle.

Osteopontin (OPN), which is a multifunctional matricellular protein that plays important roles in tissue remodeling following injury [24,25] is highly expressed in skeletal and cardiac muscles in *mdx* mice where it induces increased levels of MMP-9 [23,26,27]. Interestingly, the expression of *OPN* and *MMP-9* is similarly high in mice with cardiotoxin (CTX)-induced muscle injury [11,28,29]. Recently, the interactions between MMP-9 and OPN, as well as the elucidation of the function of OPN in dystrophic muscle, have become an intense area of research focus.

In this study, we investigated the role of MMP-9 in different stages of dystrophic muscle, by using *MMP-9* ablation in *mdx* mice. We focused our research efforts on the elucidation of its role in chemotaxis, resolution of inflammation, and tissue remodeling in order to assess its potential as a target for treatment of DMD.

2. Materials and methods

2.1. Mice experiments

All animal experiments were approved by the Animal Experiment Committee of Shinshu University, Japan, and were carried out in accordance with the institutional guidelines. Wild-type (WT; C57BL/6J) and *Mmp9* knockout ($Mmp9^{-/-}$; B6.FVB(Cg)-$Mmp9^{tm1Tvu}$/J; C57BL/6J background) mice were purchased from the Jackson Laboratory (Bar Harbor, ME, USA). X-linked muscular dystrophy *mdx* mice (C57BL/6J-Dmd^{mdx}) were a gift from the Institute of Neuroscience, National Research Center of Neurology and Psychiatry (Tokyo, Japan). $Mmp9^{-/-}$ mice were crossed with *mdx* mice to generate *mdx*/$Mmp9^{-/-}$ mice. The mouse genotypes were confirmed by PCR analysis of mouse tail DNA. An *mdx*-amplification-resistant mutation system assay was used to identify the control and *mdx* mice [30]. $Mmp9^{-/-}$ and WT mice were identified using the primer sets suggested by Jackson Laboratory. The mice were housed in plastic cages in a temperature-controlled environment with a 12 h/12 h light/dark cycle and unlimited access to food and water. For pathological examination and biochemical analysis, mice were euthanized at 2, 4, 8, and 14 weeks, and at 1 year of age, and the tibialis anterior (TA), diaphragm, and gastrocnemius muscles were dissected. The muscles were frozen in isopentane cooled with liquid nitrogen and were stored at −80 °C before they were used for histological analysis, and protein and RNA isolation.

For CTX experiments, 100 μl of CTX (10 mM in 0.9% NaCl) (Sigma, St Louis, MO, USA) was slowly injected into the TA muscles of 14-week-old WT and $Mmp9^{-/-}$ mice using a 27-gauge needle. Mice were euthanized and muscles were collected before injection and at 24, 48, and 72 h, and 5, 14, and 28 days after injection.

2.2. Histological analysis and immunohistochemistry

Serial 6-μm cryostat sections were cut from the mid-belly of the muscle to obtain the largest cross-sectional area (CSA). Sections were placed on glass slides and air-dried. For morphometric analysis, the sections were stained with hematoxylin and eosin (H&E). To detect fibrosis, a picrosirius red staining was performed. For immunohistochemistry, the sections were blocked in 10% goat serum in phosphate-buffered saline (PBS) for 30 min, and incubated overnight at 4 °C with blocking solution that contained the primary antibodies. The sections were washed briefly with 1× PBS before incubation with the secondary antibody for 1 h at room temperature. After incubation, the sections were washed three times for 30 min with 1× PBS and mounted in VECTASHIELD medium (Vector Laboratories, Burlingame, CA, USA) containing 4′,6-diamidino-2-phenylindole (DAPI). The sections were visualized using a fluorescence microscope (Olympus, Tokyo, Japan), and digital images were captured and processed with Photoshop CS4 (Adobe, San Jose, CA, USA) to optimize brightness, contrast, and resolution. The antibodies used for immunohistochemical staining in this study were as follows: Alexa Fluor 568-conjugated rat monoclonal anti-CD206 antibody (1:200; BioLegend, San Diego, CA, USA) was used for direct immunofluorescence staining. Rat monoclonal anti-CD11b (1:200; BD Transduction Laboratories, San Jose, CA, USA) and rabbit polyclonal anti-MMP-9 (1:1000; Abcam, Cambridge, UK) primary antibodies and Alexa Fluor 488- or Alexa Fluor 568-conjugated (1:500; Life Technologies, Grand Island, NY, USA) secondary antibodies were used for indirect immunofluorescence staining. Rat monoclonal anti-CD11b (1:200; BD Transduction Laboratories) and rat monoclonal anti-Ly6G (1:50; BD Transduction Laboratories) antibodies were detected using the VECTASTAIN ABC-HRP kit (Vector Laboratories, Burlingame, CA, USA) with diaminobenzidine (DAB) as a substrate, according to the manufacturer's instructions. Rabbit polyclonal anti-OPN (1:300; Rockland Immunochemical, Gilbertsville, PA, USA) was detected using the VECTASTAIN ABC-AP kit with Vector Red substrate (Vector Laboratories). Necrotic fibers were identified by immunostaining with Alexa 488-conjugated goat anti-mouse IgG antibody (1:2000; Molecular Probes or Life Technologies).

2.3. Morphometric analysis

Morphometric analysis was performed by determining the CSA of the perinuclear and the centronuclear muscle fibers in the H&E-stained TA muscle sections. Necrotic fibers, if present, were omitted from the analysis. The CSAs were examined using ImageJ software (National Institutes of Health, Bethesda, MD, USA): For each muscle, fiber boundaries were determined to evaluate the size and number of the fibers; 1709 to 2523 fibers were analyzed for each genotype. All images were obtained under identical conditions and at the same magnification. To create the CSA histograms, histological parameters were evaluated and analyzed as previously described [31].

2.4. Total protein extraction and Western blotting

Muscle protein extraction and Western blot analysis were performed as previously described [32]. Rabbit polyclonal anti-myeloperoxidase (MPO) (1:3000; Millipore, Billerica, MA, USA), rabbit

polyclonal anti-MyoD (1:3000; Santa Cruz Biotechnology, Santa Cruz, CA, USA), goat polyclonal anti-OPN (1:3000; Novocastra, Leica Microsystems, New Castle, UK), rabbit polyclonal anti-collagen type I (1:1000; Abcam), mouse monoclonal anti-collagen type IV (1:1000; Santa Cruz Biotechnology), and rabbit polyclonal anti-transforming growth factor-β (TGF-β) (1:3000; Cell Signaling Technology, Danvers, MA, USA) primary antibodies and peroxidase-conjugated secondary antibody (Bio-Rad Laboratories, Hercules, CA, USA) were used. The ECL system (GE Healthcare Life Sciences, Little Chalfont, UK) was used for Western blotting.

2.5. Gelatin zymography

Frozen tissues were homogenized in extraction buffer (62.5 mM Tris–HCl [pH 6.8], 2% sodium dodecyl sulfate [SDS], and 10% glycerol), and total protein content was assessed using a BCA protein assay kit (Bio-Rad). A gelatin zymography kit (Invitrogen, Carlsbad, CA, USA) was used to detect gelatinolytic activity. Protein extracts (50 μg) were mixed with loading buffer and separated by electrophoresis in a gelatin-containing SDS polyacrylamide gel. The gel was washed with regenerating buffer and subsequently incubated for 24 h at 37 °C in developing buffer. The gels were stained with Coomassie brilliant blue (CBB) and destained with a destaining solution (Bio-Rad). Gelatinolytic activity was identified as clear bands on a blue background. Gelatin zymography detects the activity of both the active and the pro-form of gelatinolytic MMPs, as exposure to SDS activates the pro-form MMPs without proteolytic cleavage of the prodomain. Equal protein loading was confirmed by the CBB staining. Myosin heavy chain (MHC) was used as a loading control.

2.6. RNA isolation and quantitative reverse transcriptase (qRT)-PCR

Total RNA from frozen muscle tissues was isolated using the RNeasy Fibrous Tissue Mini Kit (Qiagen, Hilden, Germany) according to the manufacturer's instructions. RNA was reverse-transcribed into cDNA using the PrimeScript RT reagent Kit with gDNA Eraser (TaKaRa Bio, Shiga, Japan). mRNA and 18S ribosomal RNA (18S rRNA) expression levels were quantified by using the KOD SYBR qPCR Mix (Toyobo, Osaka, Japan) with 10 nM of each primer in a final volume of 10 μl. The amplification reactions were carried out in duplicate on a StepOnePlus Real Time PCR system (Applied Biosystems, Foster City, CA). The thermal cycling conditions used for all primers were as follows: 2 min at 98 ° C, 40 cycles of 10 s at 98 ° C, 10 s at 60 ° C, 30 s at 68 ° C, and a final extension of 10 min at 72 ° C. Per gene, expression in all samples was quantified simultaneously. 18S rRNA was used for normalization of target gene expression. The primer sequences used for qRT-PCR are shown in the Supplemental Table S1.

2.7. Hanging wire tests

Mice at 8 weeks and 1 year of age were subjected to a hanging wire test using a 2-mm diameter metal wire apparatus suspended 35 cm above the base. The wire test was made up of three trials, with each trial consisting of an unlimited hanging period followed by a 1-min pause. The hanging time was recorded for each trial as the time from the initial grip of the wire with the two forelimbs until the mouse completely released its grip and fell down. The maximum holding impulse was calculated as follows: holding impulse (s · g) = maximum hanging time (s) × body mass (g) [33], and was used as a measure of the tension created by the body weight.

2.8. Creatine kinase activity assay

Blood was collected immediately after the animals were euthanized via the inferior vena cava using a 23-gauge needle on a 1-ml syringe, and serum was prepared by centrifugation (1500 ×*g*, 10 min, 4 °C) The serum creatine kinase (CK) level was determined by using a commercial CK reagent kit (Kanto chemical, Tokyo, Japan).

2.9. Hydroxyproline assay

Collagen and elastin contents of the diaphragm tissues of 1-year-old mice were evaluated by measuring hydroxyproline using a commercial assay kit according to the manufacturer's instructions (BioVision, San Francisco, CA, USA).

2.10. Statistical analysis

Data are expressed as the mean ± SEM. Statistical analysis was performed using unpaired *t*-tests for two-group comparisons, and one-way ANOVA with Bonferroni correction for multiple comparisons. *P*-values < 0.05 were considered significant. Statistical analyses were carried out using the GraphPad Prism version 5.0 software (GraphPad Software, Point Richmond, CA, USA).

3. Results

3.1. Characterization of *mdx*/*Mmp9*$^{-/-}$ mice

Mmp9$^{-/-}$ mice were previously reported to display a smaller muscle fiber size than WT mice [34]. We confirmed this by histological and morphometrical analysis of the TA muscles and diaphragms of WT and *Mmp9*$^{-/-}$ mice at 4 and 14 weeks of age (Supplementary Fig. S1). To elucidate the role of MMP-9 in dystrophin-deficient mice, we generated *mdx*/*Mmp9*$^{-/-}$ mice and subjected them to various analyses. Similar to *Mmp9*$^{-/-}$ mice [5], *mdx*/*Mmp9*$^{-/-}$ mice displayed normal fertility, but their body weight was significantly lower than that of *mdx* mice at 4–8 weeks and at 1 year of age (Supplementary Fig. S2). Gelatin zymography of the gastrocnemius skeletal muscle of 8-week-old WT, *Mmp9*$^{-/-}$, *mdx*, and *mdx*/*Mmp9*$^{-/-}$ mice showed that pro-MMP-9 activity was detectable only in the *mdx* skeletal muscle (Supplementary Fig. S3a). Pro-MMP-2 activity was higher in both *mdx* and *mdx*/*Mmp9*$^{-/-}$ mice than in WT mice. *MMP-2* expression was lower in *mdx*/*Mmp9*$^{-/-}$ than in *mdx* mice at 4 weeks of age (Supplementary Fig. S3b). The relative expression of the gene encoding the tissue inhibitor of metalloproteinase 1 (TIMP-1), an intrinsic MMP-9 inhibitor, was higher in *mdx*/*Mmp9*$^{-/-}$ mice than in *mdx* mice at 4 and 8 weeks of age (Supplementary Fig. S3c). The relative expression of the gene encoding TIMP-2, an inhibitor of MMP-2, was significantly higher in *mdx*/*Mmp9*$^{-/-}$ than in *mdx* mice at 1 year of age (Supplementary Fig. S3d). The relative expression of the gene encoding TIMP-3, an inhibitor of both MMP-2 and MMP-9, was significantly higher in *mdx*/*Mmp9*$^{-/-}$ than in *mdx* mice at 2 and 8 weeks, and 1 year of age (Supplementary Fig. S3e). These results suggest that an imbalance in MMP and TIMP expression might enhance the overexpression of MMP-9 in *mdx* skeletal muscle.

3.2. Effects of MMP-9 ablation on the dystrophic pathology in mdx mice

Mdx mice were reported to display an acute onset of myofiber necrosis around 3 weeks of age, a low level of chronic damage by 8 weeks of age, and a progressive replacement of muscle by fibroadipose tissue and myofiber atrophy after 6 months of age [35]. First, we performed a histological analysis of the TA and diaphragm skeletal muscles of WT, *Mmp9*$^{-/-}$, *mdx*, and *mdx*/*Mmp9*$^{-/-}$ mice at 4 and 14 weeks, and 1 year of age. While there was no apparent difference in the H&E staining of TA and diaphragm tissues between *mdx* and *mdx*/*Mmp9*$^{-/-}$ mice at 4 weeks of age (Fig. 1a), the numbers of infiltrated inflammatory cells in both muscle tissues were definitely lower in *mdx*/*Mmp9*$^{-/-}$ than in *mdx* mice at 14 weeks of age (Fig. 1b). The necrotic area, as determined by immunofluorescent staining of immunoglobulin G (IgG), was smaller in *mdx*/*Mmp9*$^{-/-}$ mice than in *mdx* mice between 4 and 14 weeks of age (Supplementary Fig. S4). In addition, the fraction of centronuclear fibers

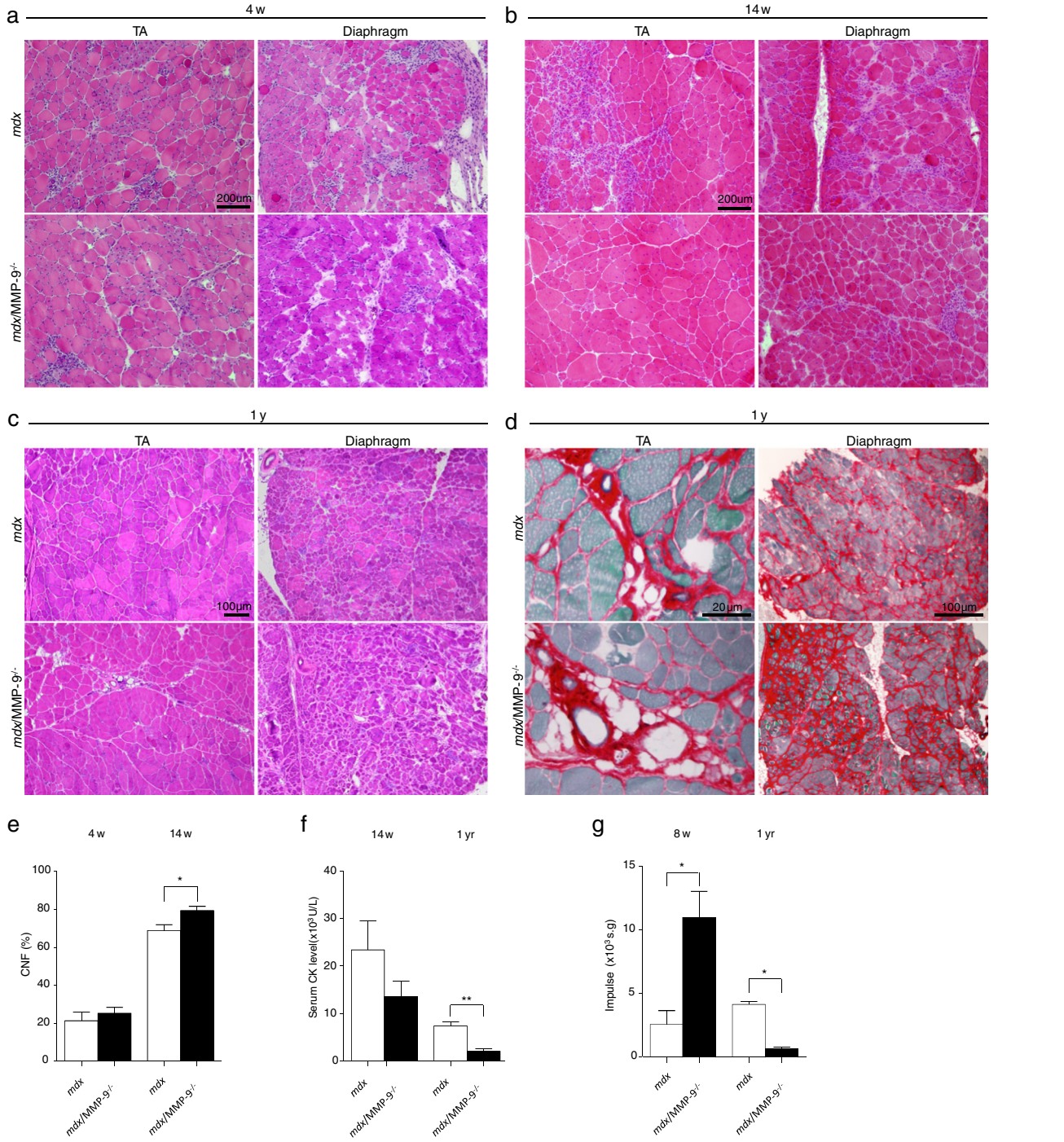

Fig. 1. MMP-9 ablation rescues *mdx* pathology at 14 weeks of age and promotes muscle regeneration in the early disease stage, but prevents the accumulation of fibroadipose tissues and is associated with decreased muscle mass and strength at 1 year of age. a, b) Histology of TA muscle and diaphragm cryosections stained with H&E from *mdx* and *mdx*/*Mmp9*$^{-/-}$ mice at 4 (a) and 14 (b) weeks of age. Scale bar: 200 μm. c) Histology of TA muscle and diaphragm cryosections stained with H&E from *mdx* and *mdx*/*Mmp9*$^{-/-}$ mice at 1 year of age. Scale bar: 100 μm. d) Picrosirius red staining of TA muscle and diaphragm from *mdx*/*Mmp9*$^{-/-}$ and *mdx* mice at 1 year of age. Scale bar: 20 μm (left panels), 100 μm (right panels). e) Fraction (%) of centronucleated fibers in TA muscle of *mdx* and *mdx*/*Mmp9*$^{-/-}$ mice at 4 and 14 weeks of age. f) Serum CK levels of *mdx* and *mdx*/*Mmp9*$^{-/-}$ mice at 4, 8, and 14 weeks of age. g) Maximum holding impulse score obtained by a hanging wire test for *mdx* and *mdx*/*Mmp9*$^{-/-}$ mice at 1 year of age. Data are presented as mean ± SEM ($n = 3$ per group). $^{*}P < 0.05$, $^{**}P < 0.01$.

(CNFs) was significantly higher in *mdx*/*Mmp9*$^{-/-}$ mice than in *mdx* mice at 14 weeks (Fig. 1e), suggesting that muscle regeneration was promoted by the ablation of MMP-9. The fiber size of the CNFs and the perinuclear fibers (PNFs) was determined for *mdx* and *mdx*/*Mmp9*$^{-/-}$ mice at 4 and 14 weeks of age. No difference was found between the genotypes of 4-week-old mice (Supplementary Fig. S5a and b). However, at 14 weeks, the CNFs of *mdx*/*Mmp9*$^{-/-}$ mice were smaller than those of *mdx* mice (Supplementary Fig. S5c and d).

As for the skeletal muscle pathology in older mice, H&E staining and picrosirius red staining of the TA muscle and of the diaphragm from 1-year-old mice showed a higher accumulation of interstitial fibroadipose tissue in *mdx*/*Mmp9*$^{-/-}$ mice than in *mdx* mice (Fig. 1c

and d). The serum CK level, a marker for muscle damage that depends on the muscle mass, was lower in *mdx*/*Mmp9*$^{-/-}$ than in *mdx* mice at 14 weeks of age; however, the difference was not significant. At 1 year of age, the CK level was significantly reduced in *mdx*/*Mmp9*$^{-/-}$ compared to *mdx* mice (Fig. 1f). The forelimb muscle strength of *mdx*/*Mmp9*$^{-/-}$ mice was greater than that of *mdx* mice at 8 weeks of age, but it was drastically reduced in *mdx*/*Mmp9*$^{-/-}$ compared to *mdx* mice at 1 year of age (Fig. 1g).

Next, we examined whether MMP-9 ablation in the *mdx* mice affected the processing of β-DG in the skeletal muscle. The β-DG immunoreactivity was lower in 8-week-old *mdx* and *mdx*/*Mmp9*$^{-/-}$ mice than in WT and *Mmp9*$^{-/-}$ mice (Supplementary Fig. S6a), and western blotting showed that the full-length 43-kDa β-DG (β-DG$_{43}$) was cleaved into a 30-kDa form (β-DG$_{30}$) in *mdx* and *mdx*/*Mmp9*$^{-/-}$ mice (Supplementary Fig. S6b and c). The β-DG$_{30}$ to β-DG$_{43}$ expression ratio showed no difference between *mdx* and *mdx*/*Mmp9*$^{-/-}$ mice. In addition, we examined the protein levels of type IV collagen, a substrate of MMP-9 in TA muscles of 14-week-old *mdx* and *mdx*/*Mmp9*$^{-/-}$ mice. We observed no differences between the protein levels in both genotypes (Supplementary Fig. S6d and e).

3.3. MMP-9 ablation results in decreased neutrophil and M1 macrophage infiltration in an early-stage mdx mouse muscle

To determine differences in the inflammatory cell infiltration between *mdx* and *mdx*/*Mmp9*$^{-/-}$ mice, we investigated the expression of Ly6G, a marker of neutrophils, in gastrocnemius muscle of *mdx* and *mdx*/*Mmp9*$^{-/-}$ mice at 4 and 14 weeks of age. Immunohistochemical staining of muscle sections showed that Ly6G expression in *mdx*/*Mmp9*$^{-/-}$ mice was lower at 4 and 14 weeks of age (Fig. 2a). The relative expression level of *Ly6G* was significantly lower in *mdx*/*Mmp9*$^{-/-}$ than in *mdx* mice at 14 weeks of age. At 4 weeks of age, the *Ly6G* expression level was lower in *mdx*/*Mmp9*$^{-/-}$ than in *mdx* mice, but the difference was not statistically significant, probably due to the high variability of *Ly6G* expression in *mdx* mice (Fig. 2b). Western blot analysis of MPO, another marker for neutrophils showed that the protein level in *mdx*/*Mmp9*$^{-/-}$ mice was significantly lower than that in *mdx* mice at 4 weeks of age. The MPO level at 14 weeks was significantly lower than at 4 weeks of age in both mouse genotypes, but there was no difference between both genotypes (Fig. 2c).

Next, we examined the expression of the macrophage marker CD11b in *mdx* and *mdx*/*Mmp9*$^{-/-}$ mice at 4 and 14 weeks of age. CD11b-positive cells were observed at both 4 and 14 weeks of age, and their number was lower in *mdx*/*Mmp9*$^{-/-}$ than in *mdx* mice (Fig. 2a). Macrophages can be divided into two subtypes, M1 and M2, based on their activation phenotype. M1 macrophages are mainly associated with muscle degeneration, while M2 macrophages play a role in muscle regeneration in dystrophic muscle [36]. We examined the localization of M2 macrophages in *mdx* and *mdx*/*Mmp9*$^{-/-}$ mice at 4 and 14 weeks of age, using CD11b as a pan-macrophage marker and CD206 as a marker for M2 macrophages. In both genotypes, the ratio of M2 to total macrophages that invaded the tissue was lower at 14 weeks than at 4 weeks of age (Fig. 2d). In 4-week-old tissue, the ratio of M2 to total macrophages that infiltrated the tissue was larger in *mdx*/*Mmp9*$^{-/-}$ than in *mdx* mice (Fig. 2d). Furthermore, the expression level of *CD11c*, a marker for M1 macrophages, was significantly lower in *mdx*/*Mmp9*$^{-/-}$ mice than in *mdx* mice at 14 weeks of age (Fig. 2e), and the *CD206* expression level in *mdx*/*Mmp9*$^{-/-}$ mice was significantly higher at 4 weeks, but lower at 14 weeks of age than in *mdx* mice (Fig. 2f).

3.4. Association between inflammatory cell infiltration and cytokine expression

We examined the mRNA levels of the genes encoding macrophage inflammatory protein-2 (MIP-2) and monocyte chemotactic protein-1 (MCP-1) in the gastrocnemius muscle of *mdx* and *mdx*/*Mmp9*$^{-/-}$ mice. MIP-2 is a neutrophil chemokine designated as a muscle-produced cytokine (myokine), and MCP-1 is a monocyte/macrophage recruiting chemokine and myokine [37–41]. The relative *MIP-2* expression in muscles of *mdx*/*Mmp9*$^{-/-}$ mice at 4 and 14 weeks of age was significantly lower than in *mdx* mice of the same age (Fig. 3a). The *MCP-1* mRNA level in *mdx*/*Mmp9*$^{-/-}$ mice was significantly higher than in *mdx* mice at 4 weeks of age (Fig. 3b). In addition, we assessed the mRNA levels of several pro- and anti-inflammatory cytokines. The levels of *interferon-γ* (*IFN-γ*) at 4 weeks, *tumor necrosis factor-α* (*TNF-α*) at 14 weeks, and *interleukin-6* (*IL-6*) at both 4 and 14 weeks of age, were significantly lower in *mdx*/*Mmp9*$^{-/-}$ than in *mdx* mice (Fig. 3c, d, and h), which was consistent with the observed increase in the proportion of M2 macrophages. As for the anti-inflammatory cytokines, *interleukin-4* (*IL-4*) was significantly lower in *mdx*/*Mmp9*$^{-/-}$ than in *mdx* mice at 4 weeks of age (Fig. 3g), but there were no significant differences in *IL-13* and *IL-10* mRNA levels between the two mouse genotypes at either time point (Fig. 3e and f).

3.5. Promotion of muscle regeneration and growth impairment in mdx/Mmp9$^{-/-}$ mice were associated with altered expression of myogenic factors

We mentioned above that MMP-9 ablation promoted muscle regeneration, but impaired muscle growth, at the early disease stage in *mdx* mice. To determine which factors are involved in these alterations in the pathology of the *mdx*/*Mmp9*$^{-/-}$ mice, we investigated the mRNA levels of the myogenic regulatory factors *Pax3*, *Myf5*, *MyoD*, and *myogenin*, at 2, 4, 8, and 14 weeks of age. The mRNA levels of *Pax3* and *Myf5* were significantly higher in *mdx*/*Mmp9*$^{-/-}$ mice than in *mdx* mice at 4 weeks of age (supplementary Fig. S7a). Although the *MyoD* mRNA levels did not differ between *mdx*/*Mmp9*$^{-/-}$ and *mdx* mice at 4 and 14 weeks of age (Supplementary Fig. S7a), the MyoD protein level was slightly lower in *mdx*/*Mmp9*$^{-/-}$ than in *mdx* mice at 14 weeks of age (Supplementary Fig. S7b and c). The mRNA level of *myogenin* in *mdx*/*Mmp9*$^{-/-}$ mice was lower than that in *mdx* mice at 14 weeks of age (Supplementary Fig. S7a).

In addition, we assessed gene expression of the muscle growth factors *myostatin*, *follistatin*, and *insulin like growth factor* (*IGF-1*), in *mdx* and *mdx*/*Mmp9*$^{-/-}$ mice, at 4 and 14 weeks of age. No significant differences were observed in the expression of any of the growth factors between both genotypes (supplementary Fig. S7d). MMP-2 is required for the growth of regenerated muscle fibers through angiogenesis in dystrophin-deficient muscle [18,42]. Therefore, we compared the mRNA levels of the angiogenic factors *angiopoietin 1* and *2*, *VEGF receptor* (*VEGFR*) *1* and *2*, *VEGFA*, and *PECAM1* in *mdx* and *mdx*/*Mmp9*$^{-/-}$ mice at 4 and 14 weeks of age. No differences in expression of any of these genes were found between both genotypes (Supplementary Fig. S7e–g). However, *VEGFA* mRNA levels in *mdx* and *mdx*/*Mmp9*$^{-/-}$ mice were significantly lower than in WT mice at 4 and 14 weeks of age (Supplementary Fig. S7f).

3.6. MMP-9 ablation induces a transient increase in OPN at the early disease stage in mdx skeletal muscle

Because OPN contributes to the increased level of MMP-9 in skeletal muscle in *mdx* mice [23], and OPN-deficiency delays the inflammatory infiltration and the onset of muscle regeneration after injury [24], we examined the expression of OPN in gastrocnemius muscles from *mdx* and *mdx*/*Mmp9*$^{-/-}$ mice at different stages. *OPN* expression was upregulated in both the genotypes at 4 weeks of age, and interestingly, the *OPN* level was significantly higher in *mdx*/*Mmp9*$^{-/-}$ mice than in *mdx* mice at the time point, while there was no difference between *mdx*/*Mmp9*$^{-/-}$ and *mdx* mice at other ages (Fig. 4a). The expression level of the OPN receptor *CD44* was higher in *mdx*/*Mmp9*$^{-/-}$ than in *mdx* mice until 8 weeks, but lower at 14 weeks and 1 year of age, although

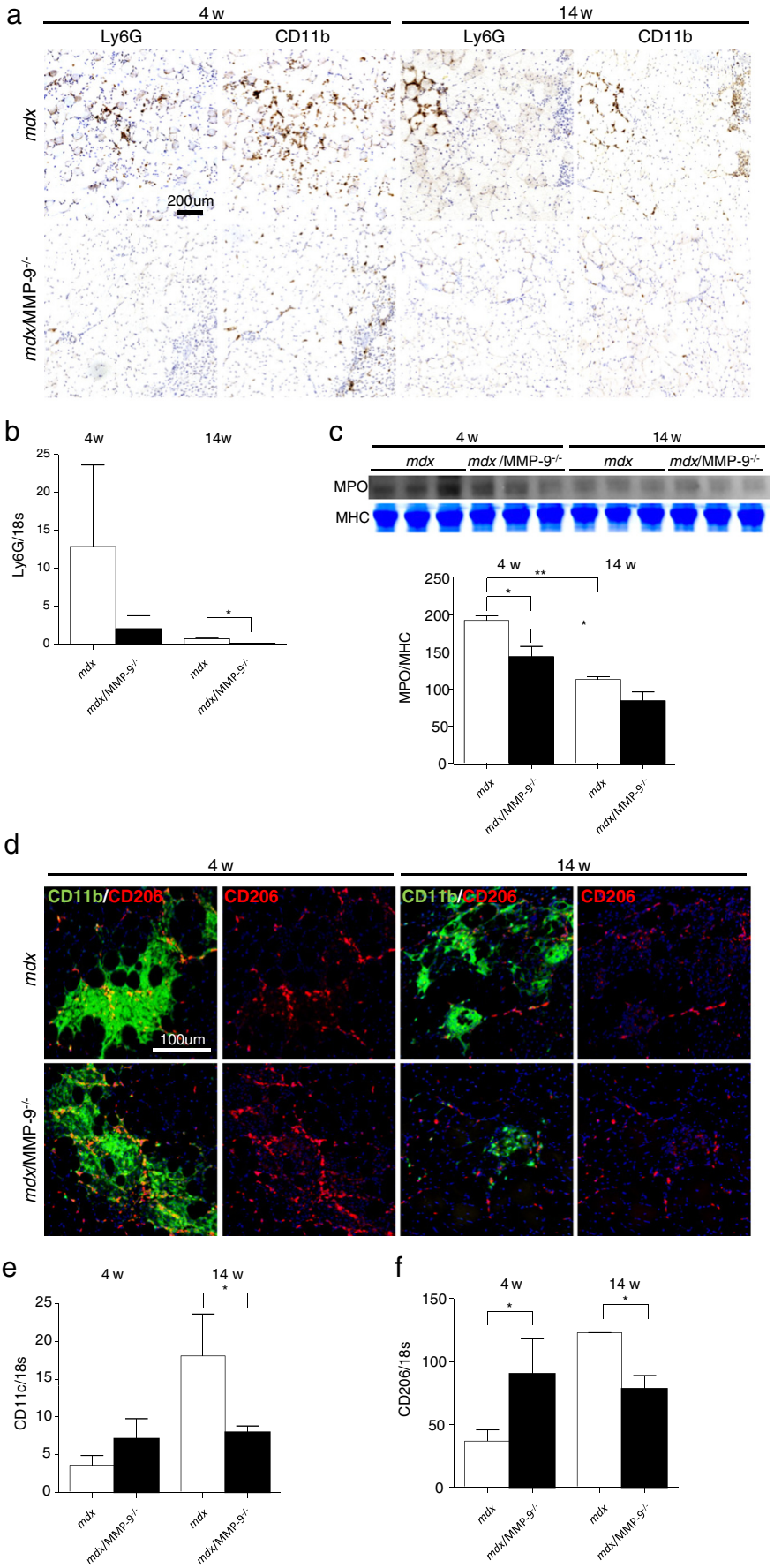
a
4 w
14 w
Ly6G
CD11b
Ly6G
CD11b
mdx
mdx/MMP-9-/-
200um
b
4w
14w
Ly6G/18s
mdx
mdx/MMP-9-/-
mdx
mdx/MMP-9-/-
c
4 w
14 w
mdx
mdx /MMP-9-/-
mdx
mdx/MMP-9-/-
MPO
MHC
4 w
14 w
MPO/MHC
mdx
mdx/MMP-9-/-
mdx
mdx/MMP-9-/-
d
4 w
14 w
CD11b/CD206
CD206
CD11b/CD206
CD206
mdx
mdx/MMP-9-/-
100um
e
4 w
14 w
CD11c/18s
mdx
mdx/MMP-9-/-
mdx
mdx/MMP-9-/-
f
4 w
14 w
CD206/18s
mdx
mdx/MMP-9-/-
mdx
mdx/MMP-9-/-

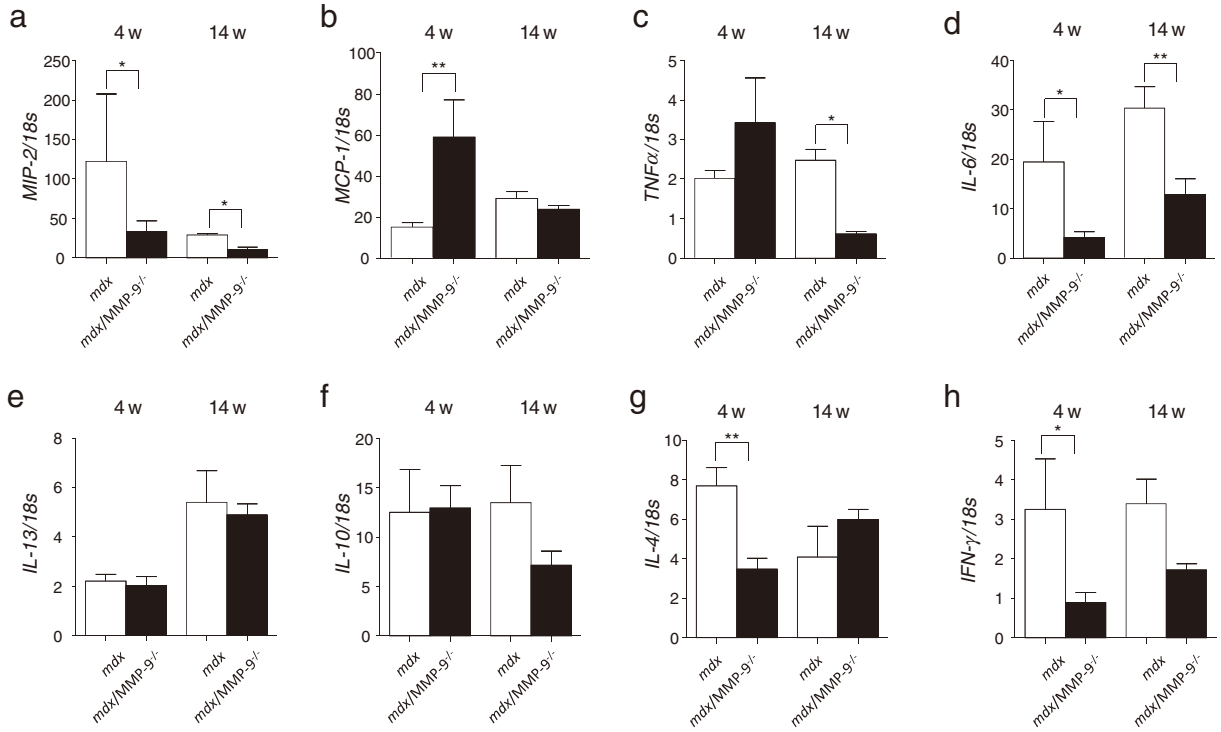

Fig. 3. Effects of MMP-9 ablation on cytokine/chemokine expression in dystrophic muscle. mRNA levels of *MIP-2* (a), *MCP-1* (b), *tumor necrosis factor α* (*TNF-α*) (c), *interleukin-6* (*IL-6*) (d), *interleukin-13* (*IL-13*) (e), *interleukin-10* (*IL-10*) (f), *interleukin-4* (*IL-4*) (g), *interferon-γ* (*IFN-γ*) (h) in the gastrocnemius muscles of *mdx* and *mdx*/*Mmp9*$^{-/-}$ at 4 and 14 weeks of age (relative to *18S rRNA*). Data are presented as mean ± SEM ($n = 3$ per group). $^{*}P < 0.05$, $^{**}P < 0.01$.

the difference was statistically significant only at 14 weeks of age (Fig. 4b). In accordance with the mRNA data, immunohistochemical staining showed that the expression of OPN was prominently upregulated in *mdx*/*Mmp9*$^{-/-}$ mice at 4 weeks of age compared to *mdx* mice, but there was no difference in expression between genotypes at 14 weeks and 1 year of age (Fig. 4c). The protein levels of both the full length (66 kDa) and the 32-kDa processed form of OPN were significantly higher in *mdx*/*Mmp9*$^{-/-}$ mice at 4 weeks, but lower at 14 weeks of age, than in *mdx* mice (Fig. 4d–f).

3.7. Cardiotoxin (CTX) injury induces a decrease in neutrophils and MIP-2 expression and an increase in macrophages and MCP-1 expression in muscles of *Mmp9*$^{-/-}$ mice

To determine whether the changes in the infiltrated inflammatory cells were related to the deficiency in MMP-9, we compared the leukocyte influx in TA muscles between WT and *Mmp9*$^{-/-}$ mice, at 24, 48, and 72 h, and 5 days after CTX injection. The H&E staining showed no significant difference between these two genotypes (Fig. 5a). However, the number of Ly6G-positive cells infiltrated in WT muscle showed larger than in *Mmp9*$^{-/-}$ at 24 h after CTX injury, increasing until 48 h. While these cells decreased rapidly from the point of 24 h after injury in *Mmp9*$^{-/-}$ mice (Fig. 5b). The *Ly6G* expression level in *Mmp9*$^{-/-}$ mice was significantly lower than that in WT at 24 h after CTX injection (Fig. 6a). The number of CD11b-positive macrophages increased gradually until 72 h after CTX injury in WT mice, while in *Mmp9*$^{-/-}$ mice, it dramatically increased at 72 h (Fig. 5c). The peak level of *CD11c* at 24 h after injury was lower in *Mmp9*$^{-/-}$ than in WT mice (Fig. 6b), while the *CD206* expression level increased until 48 h after CTX injection in both genotypes, with a higher maximum level in *Mmp9*$^{-/-}$ than in WT mice (Fig. 6c).

Further, we examined the mRNA levels of *MIP-2* and *MCP-1* in TA muscle at 24, 48, and 72 h, and 5, 14, and 28 days after CTX injury. The *MIP-2* expression in both WT and *Mmp9*$^{-/-}$ mice peaked significantly at 24 h after injury, albeit at a significantly higher level in WT than in *Mmp9*$^{-/-}$ mice (Fig. 6d). The *MCP-1* levels in both WT and *Mmp9*$^{-/-}$ mice similarly peaked at 24 h after injury, but decreased gradually at later time points, and the expression level at 24 h was significantly higher in *Mmp9*$^{-/-}$ mice than in WT mice (Fig. 6e). In accordance with previously reported results [28,29], the *OPN* expression increased dramatically upon CTX injury in muscle tissues from both genotypes. However, the expression in *Mmp9*$^{-/-}$ mice peaked at 48 h after injury and was significantly higher than the peak level in WT mice at 24 h, suggesting that MMP-9 ablation delays the upregulation of *OPN* in injured muscles (Fig. 6f).

3.8. MMP-9 ablation leads to an increased accumulation of connective tissue in skeletal muscle, without elevated TGF-β expression, in 1-year-old *mdx* mice

To study muscle pathology in the late disease stage further, we assessed the fibrosis in the diaphragm tissue of 1-year-old mice. Immunohistochemistry showed an increase in type I collagen in the diaphragm tissue of *mdx*/*Mmp9*$^{-/-}$ mice at 1 year compared to mice at

Fig. 2. Effects of MMP-9 ablation on neutrophil and macrophage infiltration in dystrophic muscle. a) Immunohistochemical staining of Ly6G and CD11b in *mdx* and *mdx*/*Mmp9*$^{-/-}$ mice at 4 and 14 weeks of age. Scale bar: 200 μm. b) mRNA levels of *Ly6G* in *mdx* and *mdx*/*Mmp9*$^{-/-}$ mice at 4 and 14 weeks of age (relative to *18S rRNA*). c) Western blot probed for MPO in *mdx* and *mdx*/*Mmp9*$^{-/-}$ mice at 4 and 14 weeks of age (upper panel). Relative (to MHC) levels of MPO shown in upper panel (lower panel). d) Immunofluorescence of CD11b (green) and CD206 (red) in *mdx* and *mdx*/*Mmp9*$^{-/-}$ mice at 4 and 14 weeks of age. Scale bar: 100 μm. e, f) Relative (to *18S rRNA*) mRNA levels of *CD11c* (e) and *CD206* (f) in *mdx* and *mdx*/*Mmp9*$^{-/-}$ mice at 4 and 14 weeks of age. Data are presented as mean ± SEM ($n = 3$ per group). $^{*}P < 0.05$, $^{**}P < 0.01$.

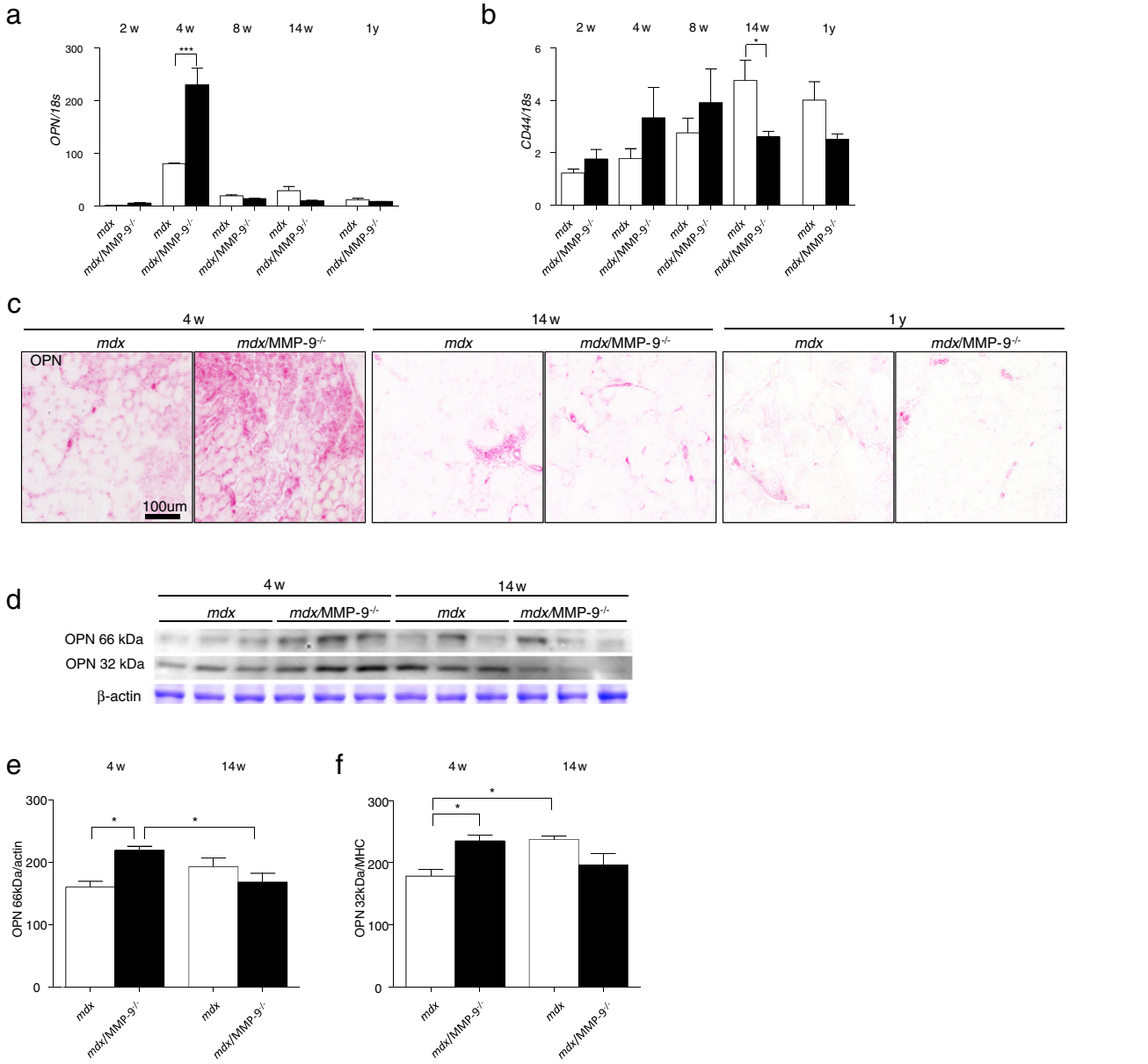

Fig. 4. Overexpression of osteopontin in skeletal muscle of *mdx* and *mdx*/*Mmp9*$^{-/-}$ mice. a and b) mRNA levels of *OPN* (a) and *CD44* (b) in the *mdx* and *mdx*/MMP-9$^{-/-}$ mice at 2, 4, 8, and 14 weeks and 1 year of age (relative to *18S rRNA*). c) Immunohistochemistry of osteopontin (OPN) in *mdx* and *mdx*/*Mmp9*$^{-/-}$ mice at 4 and 14 weeks, and 1 year of age. Scale bar: 100 μm. d, e, and f) Western blot probed for full-length 66-kDa OPN (upper bands) and cleaved 32-kDa OPN (lower bands) in *mdx* and *mdx*/*Mmp9*$^{-/-}$ mice at 4 and 14 weeks of age. Relative (to β-actin) levels of both 66 kDa OPN and 32 kDa OPN in *mdx* and *mdx*/*Mmp9*$^{-/-}$ mice at 4 and 14 weeks of age. Data are presented as mean ± SEM ($n = 3$ per group). $^{*}P < 0.05$, $^{***}P < 0.005$.

14 weeks of age. The amount of type I collagen in this genotype was higher than in 1-year-old *mdx* mice (Fig. 7a). The protein level for type I collagen, but not type IV collagen, was significantly higher in *mdx*/*Mmp9*$^{-/-}$ than in *mdx* mice at 1 year of age (Fig. 7b and c). The hydroxyproline assay showed increased connective tissue including collagen, gelatin, and elastin in the diaphragm tissue of *mdx*/*Mmp9*$^{-/-}$ compared with *mdx* mice at 1 year of age (Fig. 7d). The protein level of the 25-kDa activated form of TGF-β (TGF-β_{25}) was significantly lower in *mdx*/*Mmp9*$^{-/-}$ than in *mdx* mice, while the expression of the 50-kDa latent form of TGF-β (TGF-β_{50}) in both genotypes were at the same level at 1 year of age (Fig. 7e). The mRNA level of *TGF-β* was significantly reduced in *mdx*/*Mmp9*$^{-/-}$ relative to *mdx* mice at 14 weeks of age, but there was no difference at 1 year of age (data not shown). The mRNA levels of another fibrogenic factor, *platelet-derived growth factor* (*PDGF*), was lower in *mdx*/*Mmp9*$^{-/-}$ mice than in *mdx* mice at 1 year of age (Fig. 7f).

4. Discussion

In this study, we investigated the role of MMP-9 in skeletal muscle in the *mdx* mouse model by genetic ablation of MMP-9. Gene expression analysis of *TIMPs* and *MMP-2* in the dystrophic muscle of *mdx*/*Mmp9*$^{-/-}$ mice suggested an altered balance of expression of these proteins that might enhance the overexpression of *MMP-9* in *mdx* muscle. We showed that the ablation of *MMP-9* induced decreased muscle necrosis and augmented muscle fiber regeneration, resulting in improved muscle strength at the early disease stage, which was consistent with previously reported findings [21–23]. However, long-term MMP-9-deficiency was shown to induce an increased accumulation of adipofibrous tissue in the skeletal muscle, resulting in muscle atrophy and weakness in *mdx* mice at the late dystrophy stage. As MMP-9 was reported to cleave β-DG, which led to muscle degeneration [19,43], we assessed skeletal muscle degradation and β-DG

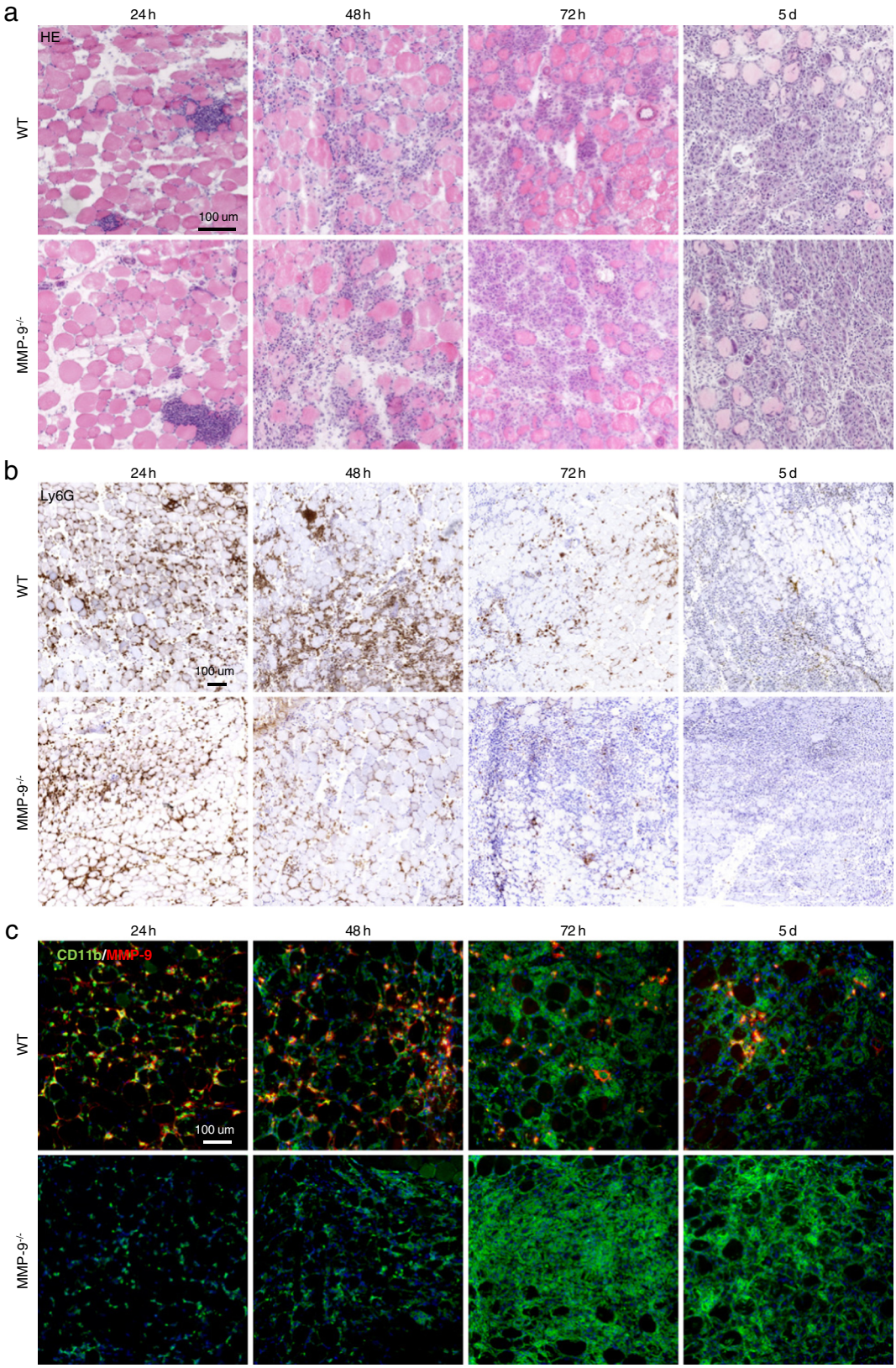

Fig. 5. MMP-9 ablation induces decreased neutrophil infiltration and increased macrophage infiltration in TA muscles following CTX injury. a-c) H&E staining (a), immunohistochemical staining of Ly6G counterstained with hematoxylin (b) and immunofluorescence of CD11b (green) and MMP-9 (red) (c) in TA muscle tissue of WT and *Mmp9*$^{-/-}$ mice at 24, 48, and 72 h, and 5 days after CTX injection. Scale bar: 100 μm.

expression in the *mdx*/*Mmp9*$^{-/-}$ mice. The cleavage of β-DG was not significantly reduced by MMP-9 ablation. We previously showed that MMP-2 did not play a role in β-DG processing in *mdx* mice [18]. Taken together, these findings imply that protease(s) other than MMP-9 and MMP-2 are responsible for β-DG processing in *mdx* mice.

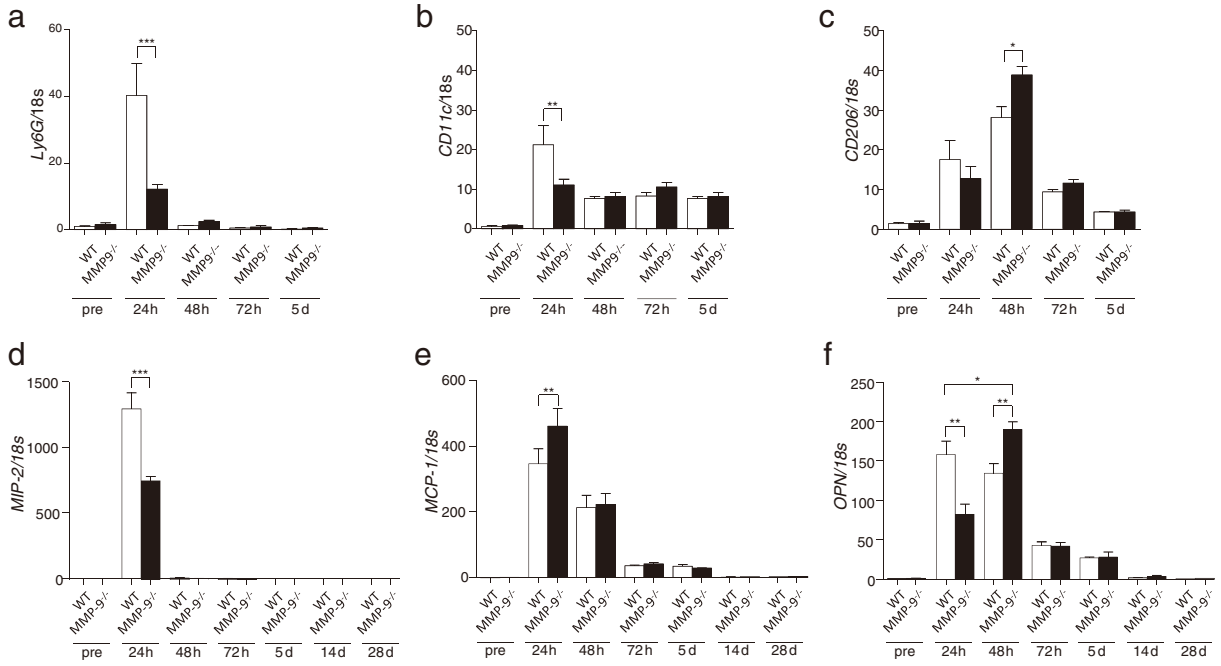

Fig. 6. MMP-9 ablation induces reduced *MIP-2* expression and increased *MCP-1* expression, and a delayed but increased *osteopontin* expression in TA muscles, following CTX injury. a-f) mRNA levels of *Ly6G* (a), *CD11c* (b), *CD206* (c), *MIP-2* (d), *MCP-1* (e), and *osteopontin* (*OPN*) (f) in TA muscle of WT and *Mmp9*$^{-/-}$ mice pre, 24, 48, and 72 h, and 5 days after CTX injection (relative to *18S rRNA*). Data are presented as mean ± SEM ($n = 4$ per group). $^{*}P < 0.05$, $^{**}P < 0.01$, $^{***}P < 0.005$.

A detailed examination of inflammatory infiltration at the early DMD stage in *mdx* and *mdx*/*Mmp9*$^{-/-}$ mice revealed reduced neutrophil infiltration, which was associated with decreased muscle necrosis and lower expression of the neutrophil recruiting chemokine *MIP-2*, in *mdx*/*Mmp9*$^{-/-}$ mice compared to *mdx* mice during the early phase of myofiber necrosis. These results are consistent with the previous finding that antibody depletion of host neutrophils ameliorates the dystrophic pathology in young *mdx* mice [44]. In contrast, *MMP-9* ablation caused an increase in macrophage infiltration with elevated expression of *MCP-1* in *mdx*/*Mmp9*$^{-/-}$ compared to *mdx* mice of the same phase. Furthermore, we observed an increase in the proportion of M2 macrophages at 4 weeks of age, which was similar to the previously reported finding of an increase in the population of M2 macrophages in strain C57BL/10 *mdx*/*Mmp9*$^{+/-}$ mice at 8 weeks of age [22]. Macrophages can play both deleterious and beneficial roles in the pathogenesis of DMD in *mdx* mice and can adopt various phenotypes in response to different stimuli [36,45]. M1 macrophages, activated by pro-inflammatory Th1 cytokines, including IFN-γ, can promote muscle fiber injury indirectly through the production of nitric oxide and inflammatory cytokines such as TNF-α and IL-6, or directly by phagocytosis [45]. Our finding that *IFN-γ* at 4 weeks, and *TNF-α* and *IL-6* at 14 weeks of age, were expressed at a significantly lower level in muscle tissues of *mdx*/*Mmp9*$^{-/-}$ than in those of *mdx* mice corroborated the relative predominance of M2 macrophage invasion in *mdx*/*Mmp9*$^{-/-}$ mice. The M2 macrophage phenotype is induced by IL-4 and IL-13 via the production of anti-inflammatory cytokines such as IL-10 [46], and reduces inflammation in the dystrophic muscle and attenuates myofiber injury in *mdx* mice [36]. Activated M2 macrophages promote muscle regeneration by stimulating the proliferation of myogenic progenitor (satellite) cells in *mdx* mice [36,45]. The modulation of the proportion of M1 and M2 macrophages can thus influence the disease course and severity of the DMD dystrophinopathy.

Neutrophils are key players in the acute phase of inflammation associated with muscle injury, but they can also exaggerate muscle damage [47,48]. In particular, MPO may play a critical role in neutrophil-mediated damage via the generation of oxidative stress [47,49]. In the process of resolution of inflammation, it is important that abrogation of the chemokine signaling blocks a continued neutrophil infiltration and that macrophages clear apoptotic neutrophils and other cells from the sites of inflammation [47,50]. Ablation of *MMP-9* was associated with decreased neutrophil infiltration and improvement of pathology in a mouse model of ischemic heart disease [51]. Furthermore, IL-8, a homologue of MIP-2, has been reported to be a substrate of MMP-9, which processes IL-8 to its active form [52]. In this study, the mechanism by which *MIP-2* expression and neutrophil infiltration in skeletal muscle were reduced in *mdx*/*Mmp9*$^{-/-}$ mice compared to *mdx* mice, was not fully investigated, however, it is likely that proteolytic activation of MIP-2 by MMP-9 might contribute to the change in chemotaxis in dystrophic muscle.

Another interesting finding in this study was that *OPN* expression in *mdx*/*Mmp9*$^{-/-}$ mice was significantly higher than in *mdx* mice during the acute phase of dystrophic pathology, at 4 weeks of age. OPN is an intriguing multifunctional protein that is highly expressed in inflammatory cells, endothelial cells, and myofibers in dystrophic and injured muscle [28,29,53] and promotes acute inflammatory influx leading to an early resolution of inflammation and muscle regeneration [24,25]. In addition, it has been reported that decreased expression of *OPN* led to greater muscle weakness in patients with DMD [54]. On the other hand, ablation of OPN in *mdx* mice resulted in reduced fibrosis and decreased muscle impairment, suggesting that chronic *OPN* overexpression is deleterious to the dystrophic muscle [26]. Therefore, transient *OPN* overexpression induced by inflammation may be beneficial for muscle regeneration, whereas chronic overexpression and processing of OPN may lead to chronic inflammation of injured muscles and eventually to fibrosis and functional impairment [25]. Hence, it is quite probable that the enhanced dynamic change in OPN expression at the early disease stage might play a part in improving the dystrophic pathology in *mdx*/*Mmp9*$^{-/-}$ mice.

We found that MMP-9 ablation in *mdx* mice promoted muscle regeneration but impaired muscle cell growth at the early stage of the dystrophy. The expression of myogenic factors involved in the early phase of muscle regeneration such as *Pax3* and *Myf5* were increased in *mdx*/*Mmp9*$^{-/-}$ mice at 4 weeks of age, while angiogenic and growth factors were not differentially expressed. MCP-1 and its receptor C-C

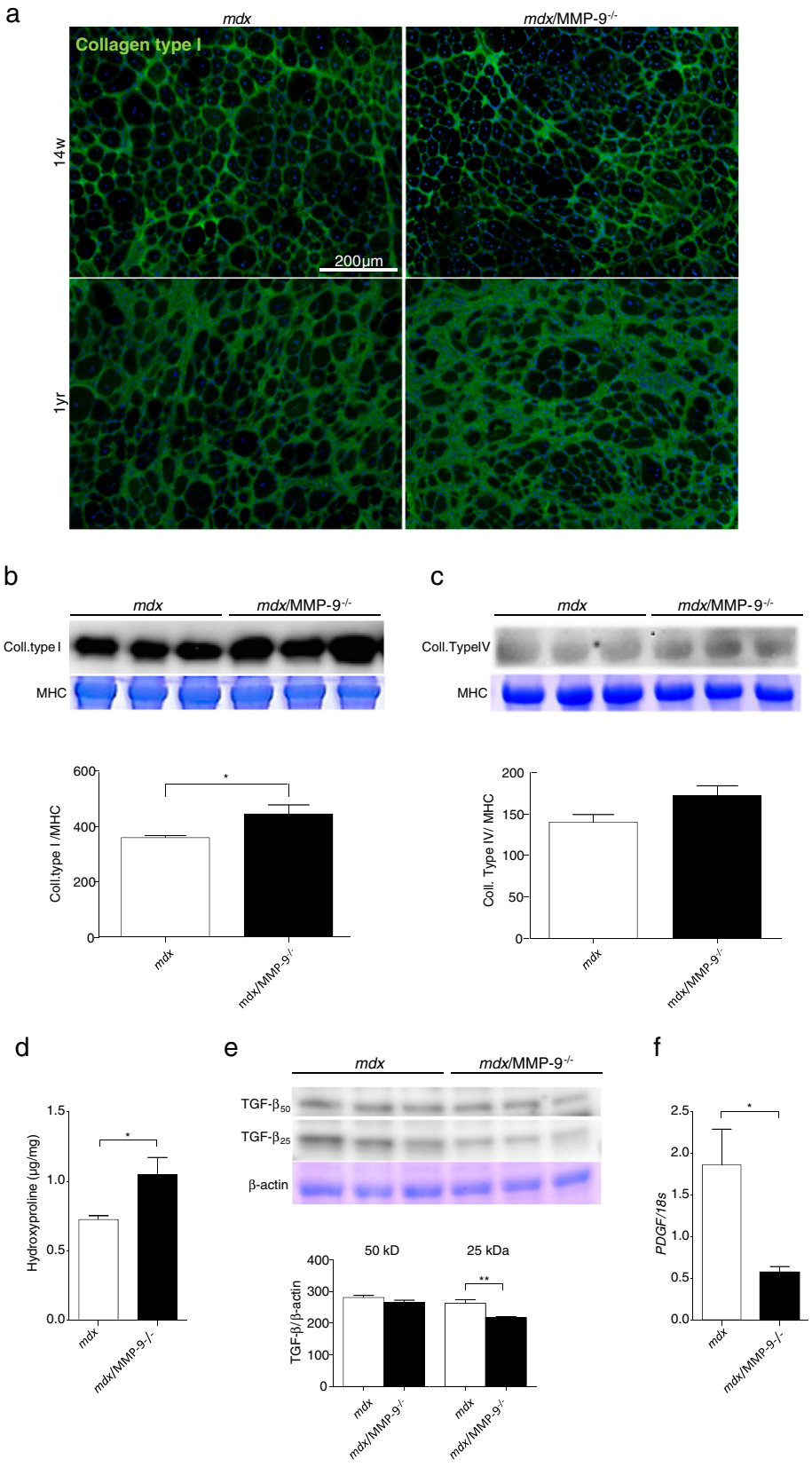

Fig. 7. MMP-9 deficiency increased fibrosis in dystrophic muscle at 1 year of age. a) Immunostaining of type I collagen in the diaphragm of *mdx* and *mdx*/*Mmp9*$^{-/-}$ at 14 weeks and 1 year of age. Scale bar: 200 μm. b, c) Western blot probed for type I collagen (b) and type IV collagen (c) in the diaphragm of *mdx* and *mdx*/*Mmp9*$^{-/-}$ mice at 1 year of age (upper panel). Relative (to MHC) protein levels shown in upper panel (lower panel). d) Quantification of tissue hydroxyproline content in the diaphragm of *mdx* and *mdx*/*Mmp9*$^{-/-}$ mice at 1 year of age. e) Western blot probed for latent form of 50-kDa TGF-β (TGF-β_{50}) and activated 25-kDa TGF-β (TGF-β_{25}) in the diaphragm of *mdx* and *mdx*/*Mmp9*$^{-/-}$ mice at 1 year of age (upper panel). Relative (to β-actin) protein levels shown in upper panel (lower panel). f) mRNA levels of *platelet-derived growth factor* (*PDGF*) in the diaphragm of *mdx* and *mdx*/*Mmp9*$^{-/-}$ mice at 1 year of age (relative to *18S rRNA*). Data are presented as mean ± SEM ($n = 3$ per group). $^{*}P < 0.05$, $^{**}P < 0.01$.

motif chemokine receptor type 2 (CCR2) have been reported to play an important role in muscle regeneration [39,55,56]. Previous studies suggested that acute and strong *OPN* expression is required for normal muscle regeneration after single severe injury [24] and that CD44, a major receptor for OPN and hyaluronan located on myoblasts, is a key regulator of myoblast migration and differentiation [57]. Therefore, the transient upregulation of these distinct myogenic factors during the acute dystrophy phase might account for the improved muscle regeneration in *mdx*/*Mmp9*$^{-/-}$ mice at this stage. Simultaneously, we observed impaired growth of the regenerated muscle in *mdx*/*Mmp9*$^{-/-}$ mice. It has been reported that MMP-9 is involved in angiogenesis, as *Mmp9*$^{-/-}$ mice demonstrated a reduction in angiogenesis [58]. We hypothesized that the correlation between the regenerated muscle growth impairment and the reduction in angiogenesis in the *mdx*/*Mmp9*$^{-/-}$ mice might allow us to identify the involved angiogenesis or growth factors. However, we found no significant differences in the mRNA levels of the examined angiogenic and growth factors in *mdx*/*Mmp9*$^{-/-}$ compared to *mdx* mice. It is conceivable that the downregulation of myogenic factors involved in late myogenesis such as MyoD and myogenin plays a role in growth impairment, and is consistent with the decreased expression levels of proinflammatory cytokines including *IL-6* and *TNF-α*, which are reported to promote regenerated fiber maturation by upregulating these myogenic factors [59], in *mdx*/*Mmp9*$^{-/-}$ mice at 14 weeks of age.

To assess whether the decrease in neutrophils and the increase in macrophages is specific to the ablation of MMP-9 with dystrophin-deficiency, we examined the histopathology of muscles injured by CTX in *Mmp9*$^{-/-}$ mice. Interestingly, neutrophil infiltration was significantly decreased compared to WT, while macrophage invasion was enhanced in *Mmp9*$^{-/-}$ mice after injury, similar to the findings in the 4-week-old *mdx*/*Mmp9*$^{-/-}$ mice. In addition, we observed a downregulation of *MIP-2* and an upregulation of *MCP-1* in the acutely injured muscle, similar to our findings in *mdx* mice at 4 week of age, which might play a role in the histopathological changes. In addition, the lack of *MMP-9* delayed the drastic upregulation of *OPN* by CTX injury observed in WT mice. The expression of *MMP-9* and *OPN* had been previously reported to transiently increase upon CTX-induced muscle injury in WT mice [11,28,29]. These findings suggest that MMP-9 might regulate *OPN* expression directly or indirectly in dystrophic, as well as in acutely injured muscle tissues.

Our study demonstrated that *mdx*/*Mmp9*$^{-/-}$ mice developed more excessive fibrosis with a significantly increased protein level of type I collagen in skeletal muscle than *mdx* mice during the later stage of disease (at 1 year). MMP-9 has been reported to degrade various fibrogenic ECM components such as collagen and proteoglycans [60–62]. On the other hand, it has been reported that MMP-9 activates TGF-β through proteolytic cleavage of the inhibitory domain [63], and that inhibition of MMP-9 reduces the active TGF-β protein level in the diaphragm of *mdx* mice at 14 weeks of age [21]. In addition, a previous study reported that ablation of MMP-9 reduced cardiac fibrosis with improved heart function in 1-year-old *mdx* mice, although TGF-β was not assessed in the study and the precise underlying mechanism remained unclear [23]. In this study, the protein level of the active form of TGF-β (25 kDa) at 1 year of age and the mRNA level of *TGF-β* at 14 weeks of age were lower in the skeletal muscle of *mdx*/*Mmp9*$^{-/-}$ mice than in *mdx* mice, consistent with the prospective reduction in activation of TGF-β. In addition, the mRNA levels of other important fibrogenic factors including *PDGF* and *OPN* (data not shown) were also lower in *mdx*/*Mmp9*$^{-/-}$ mice than in *mdx* mice at 1 year of age, suggesting that these proteins might not be directly involved in the pathology at this stage. Taken together, these results imply that MMP-9 plays an important role in degrading ECM components causing tissue fibrosis in aged *mdx* skeletal muscle. However, whether the exaggerated muscle fibrosis in aged *mdx*/*MMP9*$^{-/-}$ mice is due to prolonged inhibition of MMP-9 or a stage-specific effect of MMP-9 inhibition cannot be clarified in this study. Further experiments using a MMP-9 specific chemical inhibitor are required to distinguish the two possibilities.

In summary, we revealed that the principal role of MMP-9 in dystrophic muscle is biphasic; MMP-9 delays the resolution of inflammation and exacerbates the dystrophic pathology in the early disease stage, while in the later stage, MMP-9 plays a critical role in suppressing the accumulation of fibroadipose tissue. It is known that corticosteroids increase muscle strength in DMD patients [64], and that MMP-9 is inhibited by corticosteroids [65,66]. Therefore, MMP-9 could be a promising therapeutic target for the treatment of DMD; however, it is important to carefully consider the disease stage and conditions before clinical application.

Transparency document

The Transparency document associated with this article can be found, in the online version.

Conflict of interest

The authors declare no conflict of interest.

Acknowledgments

This research was supported by JSPS KAKENHI (21300157 to AN and 26860792 to NS).

Appendix A. Supplementary data

Supplementary data to this article can be found online at http://dx.doi.org/10.1016/j.bbadis.2015.07.008.

References

[1] K. Bushby, R. Finkel, D.J. Birnkrant, L.E. Case, P.R. Clemens, L. Cripe, A. Kaul, K. Kinnett, C. McDonald, S. Pandya, J. Poysky, F. Shapiro, J. Tomezsko, C. Constantin, Diagnosis and management of Duchenne muscular dystrophy, part 1: diagnosis, and pharmacological and psychosocial management, Lancet Neurol. 9 (2010) 77–93.
[2] E.P. Hoffman, R.H. Brown Jr., L.M. Kunkel, Dystrophin: the protein product of the Duchenne muscular dystrophy locus, Cell 51 (1987) 919–928.
[3] K.P. Campbell, S.D. Kahl, Association of dystrophin and an integral membrane glycoprotein, Nature 338 (1989) 259–262.
[4] K.E. Davies, K.J. Nowak, Molecular mechanisms of muscular dystrophies: old and new players, Nat. Rev. Mol. Cell Biol. 7 (2006) 762–773.
[5] T.H. Vu, J.M. Shipley, G. Bergers, J.E. Berger, J.A. Helms, D. Hanahan, S.D. Shapiro, R.M. Senior, Z. Werb, MMP-9/gelatinase B is a key regulator of growth plate angiogenesis and apoptosis of hypertrophic chondrocytes, Cell 93 (1998) 411–422.
[6] A. Page-McCaw, A.J. Ewald, Z. Werb, Matrix metalloproteinases and the regulation of tissue remodelling, Nat. Rev. Mol. Cell Biol. 8 (2007) 221–233.
[7] J.R. Sanes, The basement membrane/basal lamina of skeletal muscle, J. Biol. Chem. 278 (2003) 12601–12604.
[8] M. Kjaer, Role of extracellular matrix in adaptation of tendon and skeletal muscle to mechanical loading, Physiol. Rev. 84 (2004) 649–698.
[9] P. Van Lint, C. Libert, Chemokine and cytokine processing by matrix metalloproteinases and its effect on leukocyte migration and inflammation, J. Leukoc. Biol. 82 (2007) 1375–1381.
[10] A. Kumar, S. Bhatnagar, Matrix metalloproteinase inhibitor batimastat alleviates pathology and improves skeletal muscle function in dystrophin-deficient mdx mice, Am. J. Pathol. 177 (2010) 248–260.
[11] S. Kherif, C. Lafuma, M. Dehaupas, S. Lachkar, J.G. Fournier, M. Verdiere-Sahuque, M. Fardeau, H.S. Alameddine, Expression of matrix metalloproteinases 2 and 9 in regenerating skeletal muscle: a study in experimentally injured and mdx muscles, Dev. Biol. 205 (1999) 158–170.
[12] A. Nakamura, K. Yoshida, H. Ueda, S. Takeda, S. Ikeda, Up-regulation of mitogen activated protein kinases in mdx skeletal muscle following chronic treadmill exercise, Biochim. Biophys. Acta 1740 (2005) 326–331.
[13] K. Fukushima, A. Nakamura, H. Ueda, K. Yuasa, K. Yoshida, S. Takeda, S. Ikeda, Activation and localization of matrix metalloproteinase-2 and −9 in the skeletal muscle of the muscular dystrophy dog (CXMDJ), BMC Musculoskelet. Disord. 8 (2007) 54.
[14] V.D. Nadarajah, M. van Putten, A. Chaouch, P. Garrood, V. Straub, H. Lochmuller, H.B. Ginjaar, A.M. Aartsma-Rus, G.J. van Ommen, J.T. den Dunnen, P.A. t Hoen, Serum matrix metalloproteinase-9 (MMP-9) as a biomarker for monitoring disease progression in Duchenne muscular dystrophy (DMD), Neuromuscul. Disord. 21 (2011) 569–578.
[15] T.H. Vu, Z. Werb, Matrix metalloproteinases: effectors of development and normal physiology, Genes Dev. 14 (2000) 2123–2133.

[16] J.D. Mott, Z. Werb, Regulation of matrix biology by matrix metalloproteinases, Curr. Opin. Cell Biol. 16 (2004) 558–564.
[17] H.S. Alameddine, Matrix metalloproteinases in skeletal muscles: friends or foes? Neurobiol. Dis. 48 (2012) 508–518.
[18] D. Miyazaki, A. Nakamura, K. Fukushima, K. Yoshida, S. Takeda, S. Ikeda, Matrix metalloproteinase-2 ablation in dystrophin-deficient mdx muscles reduces angiogenesis resulting in impaired growth of regenerated muscle fibers, Hum. Mol. Genet. 20 (2011) 1787–1799.
[19] H. Yamada, F. Saito, H. Fukuta-Ohi, D. Zhong, A. Hase, K. Arai, A. Okuyama, R. Maekawa, T. Shimizu, K. Matsumura, Processing of beta-dystroglycan by matrix metalloproteinase disrupts the link between the extracellular matrix and cell membrane via the dystroglycan complex, Hum. Mol. Genet. 10 (2001) 1563–1569.
[20] D. Zhong, F. Saito, Y. Saito, A. Nakamura, T. Shimizu, K. Matsumura, Characterization of the protease activity that cleaves the extracellular domain of beta-dystroglycan, Biochem. Biophys. Res. Commun. 345 (2006) 867–871.
[21] H. Li, A. Mittal, D.Y. Makonchuk, S. Bhatnagar, A. Kumar, Matrix metalloproteinase-9 inhibition ameliorates pathogenesis and improves skeletal muscle regeneration in muscular dystrophy, Hum. Mol. Genet. 18 (2009) 2584–2598.
[22] S.M. Hindi, J. Shin, Y. Ogura, H. Li, A. Kumar, Matrix metalloproteinase-9 inhibition improves proliferation and engraftment of myogenic cells in dystrophic muscle of mdx mice, PLoS One 8 (2013) e72121.
[23] S. Dahiya, S. Givvimani, S. Bhatnagar, N. Qipshidze, S.C. Tyagi, A. Kumar, Osteopontin-stimulated expression of matrix metalloproteinase-9 causes cardiomyopathy in the mdx model of Duchenne muscular dystrophy, J. Immunol. 187 (2011) 2723–2731.
[24] K. Uaesoontrachoon, D.K. Wasgewatte Wijesinghe, E.J. Mackie, C.N. Pagel, Osteopontin deficiency delays inflammatory infiltration and the onset of muscle regeneration in a mouse model of muscle injury, Dis. Model. Mech. 6 (2013) 197–205.
[25] C.N. Pagel, D.K. Wasgewatte Wijesinghe, N. Taghavi Esfandouni, E.J. Mackie, Osteopontin, inflammation and myogenesis: influencing regeneration, fibrosis and size of skeletal muscle, J. Cell Commun. Signal. 8 (2014) 95–103.
[26] S.A. Vetrone, E. Montecino-Rodriguez, E. Kudryashova, I. Kramerova, E.P. Hoffman, S.D. Liu, M.C. Miceli, M.J. Spencer, Osteopontin promotes fibrosis in dystrophic mouse muscle by modulating immune cell subsets and intramuscular TGF-beta, J. Clin. Investig. 119 (2009) 1583–1594.
[27] J.D. Porter, A.P. Merriam, P. Leahy, B. Gong, J. Feuerman, G. Cheng, S. Khanna, Temporal gene expression profiling of dystrophin-deficient (mdx) mouse diaphragm identifies conserved and muscle group-specific mechanisms in the pathogenesis of muscular dystrophy, Hum. Mol. Genet. 13 (2004) 257–269.
[28] A. Hirata, S. Masuda, T. Tamura, K. Kai, K. Ojima, A. Fukase, K. Motoyoshi, K. Kamakura, Y. Miyagoe-Suzuki, S. Takeda, Expression profiling of cytokines and related genes in regenerating skeletal muscle after cardiotoxin injection: a role for osteopontin, Am. J. Pathol. 163 (2003) 203–215.
[29] E.P. Hoffman, H. Gordish-Dressman, V.D. McLane, J.M. Devaney, P.D. Thompson, P. Visich, P.M. Gordon, L.S. Pescatello, R.F. Zoeller, N.M. Moyna, T.J. Angelopoulos, E. Pegoraro, G.A. Cox, P.M. Clarkson, Alterations in osteopontin modify muscle size in females in both humans and mice, Med. Sci. Sports Exerc. 45 (2013) 1060–1068.
[30] A. Amalfitano, J.S. Chamberlain, The mdx-amplification-resistant mutation system assay, a simple and rapid polymerase chain reaction-based detection of the mdx allele, Muscle Nerve 19 (1996) 1549–1553.
[31] R. Massa, G. Silvestri, Y.C. Zeng, A. Martorana, G. Sancesario, G. Bernardi, Muscle regeneration in mdx mice: resistance to repeated necrosis is compatible with myofiber maturity, Basic Appl. Myol. 7 (1997) 387–394.
[32] A. Nakamura, M. Kobayashi, M. Kuraoka, K. Yuasa, N. Yugeta, T. Okada, S. Takeda, Initial pulmonary respiration causes massive diaphragm damage and hyper-CKemia in Duchenne muscular dystrophy dog, Sci. Rep. 3 (2013) 2183.
[33] C.G. Carlson, J. Rutter, C. Bledsoe, R. Singh, H. Hoff, K. Bruemmer, J. Sesti, F. Gatti, J. Berge, L. McCarthy, A simple protocol for assessing inter-trial and inter-examiner reliability for two noninvasive measures of limb muscle strength, J. Neurosci. Methods 186 (2010) 226–230.
[34] R.S. Mehan, B.J. Greybeck, K. Emmons, W.C. Byrnes, D.L. Allen, Matrix metalloproteinase-9 deficiency results in decreased fiber cross-sectional area and alters fiber type distribution in mouse hindlimb skeletal muscle, Cells Tissues Organs 194 (2011) 510–520.
[35] M.D. Grounds, H.G. Radley, G.S. Lynch, K. Nagaraju, A. De Luca, Towards developing standard operating procedures for pre-clinical testing in the mdx mouse model of Duchenne muscular dystrophy, Neurobiol. Dis. 31 (2008) 1–19.
[36] S.A. Villalta, H.X. Nguyen, B. Deng, T. Gotoh, J.G. Tidball, Shifts in macrophage phenotypes and macrophage competition for arginine metabolism affect the severity of muscle pathology in muscular dystrophy, Hum. Mol. Genet. 18 (2009) 482–496.
[37] B. Chazaud, C. Sonnet, P. Lafuste, G. Bassez, A.C. Rimaniol, F. Poron, F.J. Authier, P.A. Dreyfus, R.K. Gherardi, Satellite cells attract monocytes and use macrophages as a support to escape apoptosis and enhance muscle growth, J. Cell Biol. 163 (2003) 1133–1143.
[38] P.K. Shireman, V. Contreras-Shannon, S.M. Reyes-Reyna, S.C. Robinson, L.M. McManus, MCP-1 parallels inflammatory and regenerative responses in ischemic muscle, J. Surg. Res. 134 (2006) 145–157.
[39] P.K. Shireman, V. Contreras-Shannon, O. Ochoa, B.P. Karia, J.E. Michalek, L.M. McManus, MCP-1 deficiency causes altered inflammation with impaired skeletal muscle regeneration, J. Leukoc. Biol. 81 (2007) 775–785.
[40] J.M. Peterson, F.X. Pizza, Cytokines derived from cultured skeletal muscle cells after mechanical strain promote neutrophil chemotaxis in vitro, J. Appl. Physiol. 106 (2009) (1985) 130–137.
[41] B.K. Pedersen, M.A. Febbraio, Muscles, exercise and obesity: skeletal muscle as a secretory organ, Nat. Rev. Endocrinol. 8 (2012) 457–465.
[42] B. Nico, D. Mangieri, A. De Luca, P. Corsi, V. Benagiano, R. Tamma, T. Annese, V. Longo, E. Crivellato, D. Ribatti, Nerve growth factor and its receptors TrkA and p75 are upregulated in the brain of mdx dystrophic mouse, Neuroscience 161 (2009) 1057–1066.
[43] K. Matsumura, D. Zhong, F. Saito, K. Arai, K. Adachi, H. Kawai, I. Higuchi, I. Nishino, T. Shimizu, Proteolysis of beta-dystroglycan in muscular diseases, Neuromuscul. Disord. 15 (2005) 336–341.
[44] S. Hodgetts, H. Radley, M. Davies, M.D. Grounds, Reduced necrosis of dystrophic muscle by depletion of host neutrophils, or blocking TNFalpha function with Etanercept in mdx mice, Neuromuscul. Disord. 16 (2006) 591–602.
[45] J.G. Tidball, S.A. Villalta, Regulatory interactions between muscle and the immune system during muscle regeneration, Am. J. Physiol. Regul. Integr. Comp. Physiol. 298 (2010) R1173–R1187.
[46] S.A. Villalta, C. Rinaldi, B. Deng, G. Liu, B. Fedor, J.G. Tidball, Interleukin-10 reduces the pathology of mdx muscular dystrophy by deactivating M1 macrophages and modulating macrophage phenotype, Hum. Mol. Genet. 20 (2011) 790–805.
[47] J.G. Tidball, Inflammatory processes in muscle injury and repair, Am. J. Physiol. Regul. Integr. Comp. Physiol. 288 (2005) R345–R353.
[48] H. Toumi, T.M. Best, The inflammatory response: friend or enemy for muscle injury? Br. J. Sports Med. 37 (2003) 284–286.
[49] H.X. Nguyen, A.J. Lusis, J.G. Tidball, Null mutation of myeloperoxidase in mice prevents mechanical activation of neutrophil lysis of muscle cell membranes in vitro and in vivo, J. Physiol. 565 (2005) 403–413.
[50] A. Ortega-Gomez, M. Perretti, O. Soehnlein, Resolution of inflammation: an integrated view, EMBO Mol. Med. 5 (2013) 661–674.
[51] A.M. Romanic, S.M. Harrison, W. Bao, C.L. Burns-Kurtis, S. Pickering, J. Gu, E. Grau, J. Mao, G.M. Sathe, E.H. Ohlstein, T.L. Yue, Myocardial protection from ischemia/reperfusion injury by targeted deletion of matrix metalloproteinase-9, Cardiovasc. Res. 54 (2002) 549–558.
[52] P.E. Van den Steen, P. Proost, A. Wuyts, J. Van Damme, G. Opdenakker, Neutrophil gelatinase B potentiates interleukin-8 tenfold by aminoterminal processing, whereas it degrades CTAP-III, PF-4, and GRO-alpha and leaves RANTES and MCP-2 intact, Blood 96 (2000) 2673–2681.
[53] S. Zanotti, S. Gibertini, C. Di Blasi, C. Cappelletti, P. Bernasconi, R. Mantegazza, L. Morandi, M. Mora, Osteopontin is highly expressed in severely dystrophic muscle and seems to play a role in muscle regeneration and fibrosis, Histopathology 59 (2011) 1215–1228.
[54] E. Pegoraro, E.P. Hoffman, L. Piva, B.F. Gavassini, S. Cagnin, M. Ermani, L. Bello, G. Soraru, B. Pacchioni, M.D. Bonifati, G. Lanfranchi, C. Angelini, A. Kesari, I. Lee, H. Gordish-Dressman, J.M. Devaney, C.M. McDonald, SPP1 genotype is a determinant of disease severity in Duchenne muscular dystrophy, Neurology 76 (2011) 219–226.
[55] C.O. Martinez, M.J. McHale, J.T. Wells, O. Ochoa, J.E. Michalek, L.M. McManus, P.K. Shireman, Regulation of skeletal muscle regeneration by CCR2-activating chemokines is directly related to macrophage recruitment, Am. J. Physiol. Regul. Integr. Comp. Physiol. 299 (2010) R832–R842.
[56] V. Contreras-Shannon, O. Ochoa, S.M. Reyes-Reyna, D. Sun, J.E. Michalek, W.A. Kuziel, L.M. McManus, P.K. Shireman, Fat accumulation with altered inflammation and regeneration in skeletal muscle of CCR2$^{-/-}$ mice following ischemic injury, Am. J. Physiol. Cell Physiol. 292 (2007) C953–C967.
[57] E. Mylona, K.A. Jones, S.T. Mills, G.K. Pavlath, CD44 regulates myoblast migration and differentiation, J. Cell. Physiol. 209 (2006) 314–321.
[58] G. Christoffersson, E. Vagesjo, J. Vandooren, M. Liden, S. Massena, R.B. Reinert, M. Brissova, A.C. Powers, G. Opdenakker, M. Phillipson, VEGF-A recruits a proangiogenic MMP-9-delivering neutrophil subset that induces angiogenesis in transplanted hypoxic tissue, Blood 120 (2012) 4653–4662.
[59] P. Munoz-Canoves, C. Scheele, B.K. Pedersen, A.L. Serrano, Interleukin-6 myokine signaling in skeletal muscle: a double-edged sword? FEBS J. 280 (2013) 4131–4148.
[60] J.J. Tomasek, N.L. Halliday, D.L. Updike, J.S. Ahern-Moore, T.K. Vu, R.W. Liu, E.W. Howard, Gelatinase A activation is regulated by the organization of the polymerized actin cytoskeleton, J. Biol. Chem. 272 (1997) 7482–7487.
[61] I. Massova, L.P. Kotra, R. Fridman, S. Mobashery, Matrix metalloproteinases: structures, evolution, and diversification, FASEB J. 12 (1998) 1075–1095.
[62] S. Dahiya, S. Bhatnagar, S.M. Hindi, C. Jiang, P.K. Paul, S. Kuang, A. Kumar, Elevated levels of active matrix metalloproteinase-9 cause hypertrophy in skeletal muscle of normal and dystrophin-deficient mdx mice, Hum. Mol. Genet. 20 (2011) 4345–4359.
[63] Q. Yu, I. Stamenkovic, Cell surface-localized matrix metalloproteinase-9 proteolytically activates TGF-beta and promotes tumor invasion and angiogenesis, Genes Dev. 14 (2000) 163–176.
[64] A.Y. Manzur, T. Kuntzer, M. Pike, A. Swan, Glucocorticoid corticosteroids for Duchenne muscular dystrophy, Cochrane Database Syst. Rev. (2008) CD003725.
[65] C.S. De Paiva, R.M. Corrales, A.L. Villarreal, W.J. Farley, D.Q. Li, M.E. Stern, S.C. Pflugfelder, Corticosteroid and doxycycline suppress MMP-9 and inflammatory cytokine expression, MAPK activation in the corneal epithelium in experimental dry eye, Exp. Eye Res. 83 (2006) 526–535.
[66] J. Mysliwiec, M. Adamczyk, P. Pawlowski, A. Nikolajuk, M. Gorska, Serum gelatinases (MMP-2 and MMP-9) and VCAM-1 as a guideline in a therapeutic approach in Graves' ophthalmopathy, Endokrynol. Pol. 58 (2007) 105–109.

Fig. S1

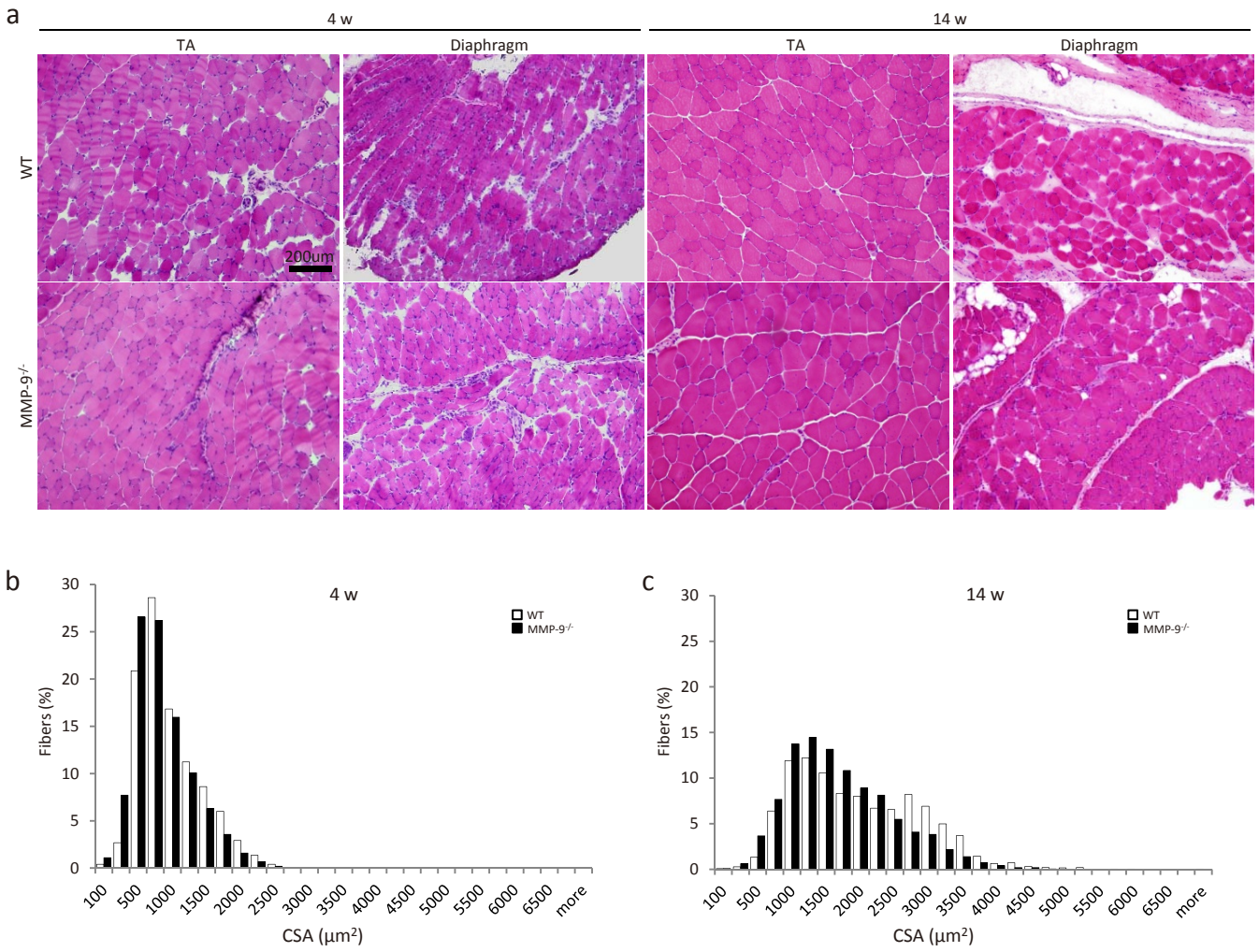

Fig. S1. Histopathological and morphometrical analysis of muscle tissues from WT and *Mmp9*$^{-/-}$ mice.

a) Histopathology of muscle cryosections stained with H&E of the TA muscle and the diaphragm of WT and *Mmp9*$^{-/-}$ mice at 4 and 14 weeks of age. Scale bar: 200 µm. b, c) Fiber size distribution in TA muscle of WT and *Mmp9*$^{-/-}$ mice at 4 weeks of age (b) and at 14 weeks of age (c) (n = 3 per group).

Fig. S2

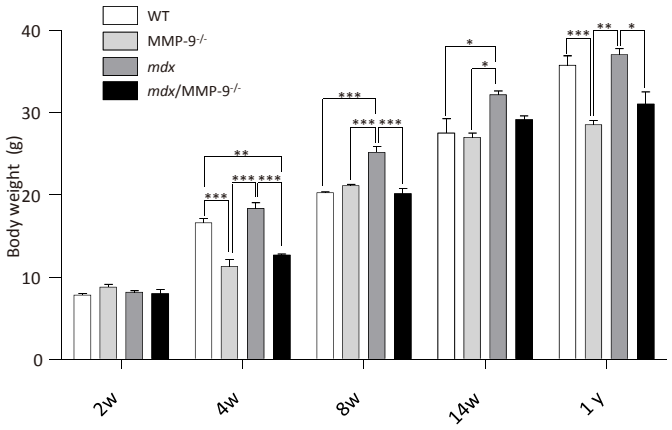

Fig. S2. Body weight of WT, *Mmp9*$^{-/-}$, *mdx*, and *mdx*/*Mmp9*$^{-/-}$ mice at 2, 4, 8, and 14 weeks, and 1 year of age (n = 3 per group).

Fig. S3

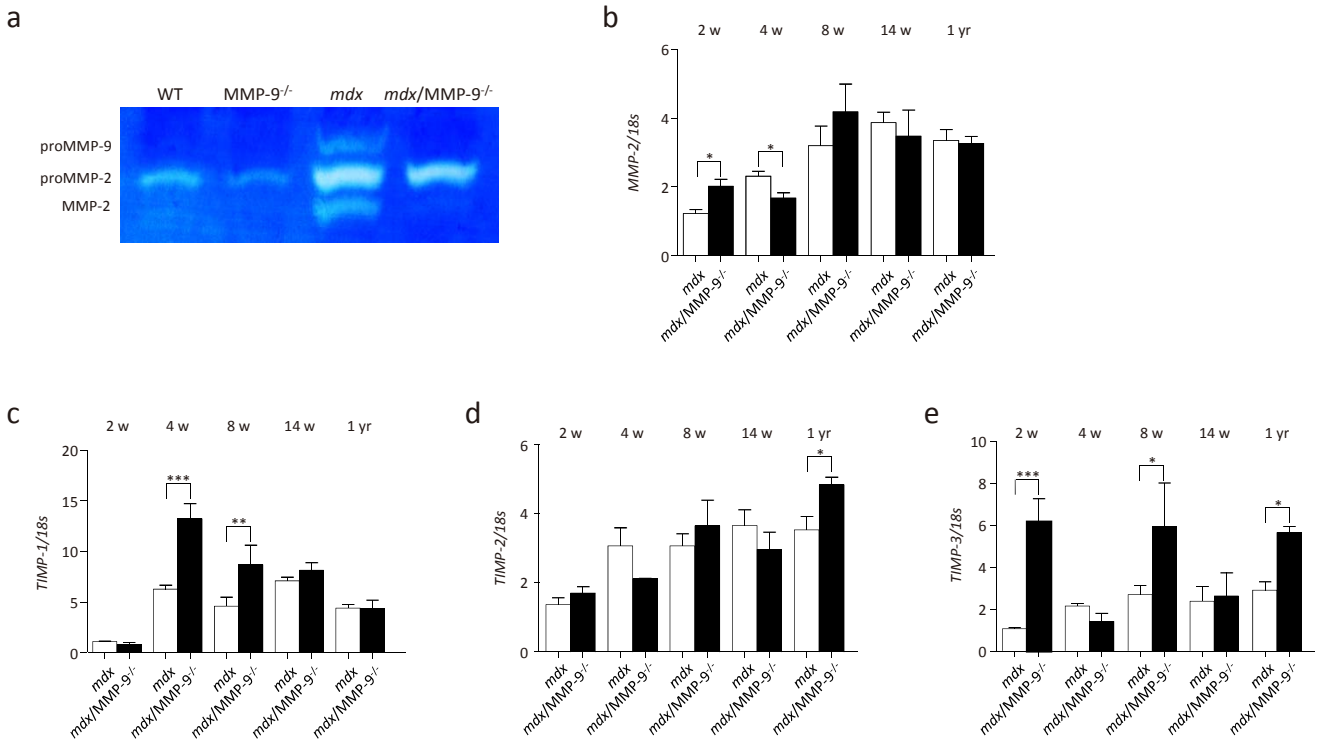

Fig. S3. MMP-9 ablation induces decreased *MMP2* expression and MMP-2 activity during the early disease stage and increased expression of *tissue inhibitor of metalloproteinase* (*TIMP*)-*1* at 4 and 8 weeks of age. a) MMP-2 and MMP-9 protein activity in the gastrocnemius muscles of WT, *Mmp9*$^{-/-}$, *mdx*, and *mdx*/*Mmp9*$^{-/-}$ mice at 8 weeks of age as determined by gelatin zymography. b-e) Relative (to *18S rRNA*) mRNA levels of *MMP-2* (b), *TIMP-1* (c), *TIMP-2* (d), and *TIMP-3* (e) in the gastrocnemius muscles of *mdx* and *mdx*/*Mmp9*$^{-/-}$ mice at 2, 4, 8, and 14 weeks, and 1 year of age. Data are presented as mean ± SEM (n = 3 per group). *$P < 0.05$, **$P < 0.01$, ***$P < 0.005$.

Fig. S4

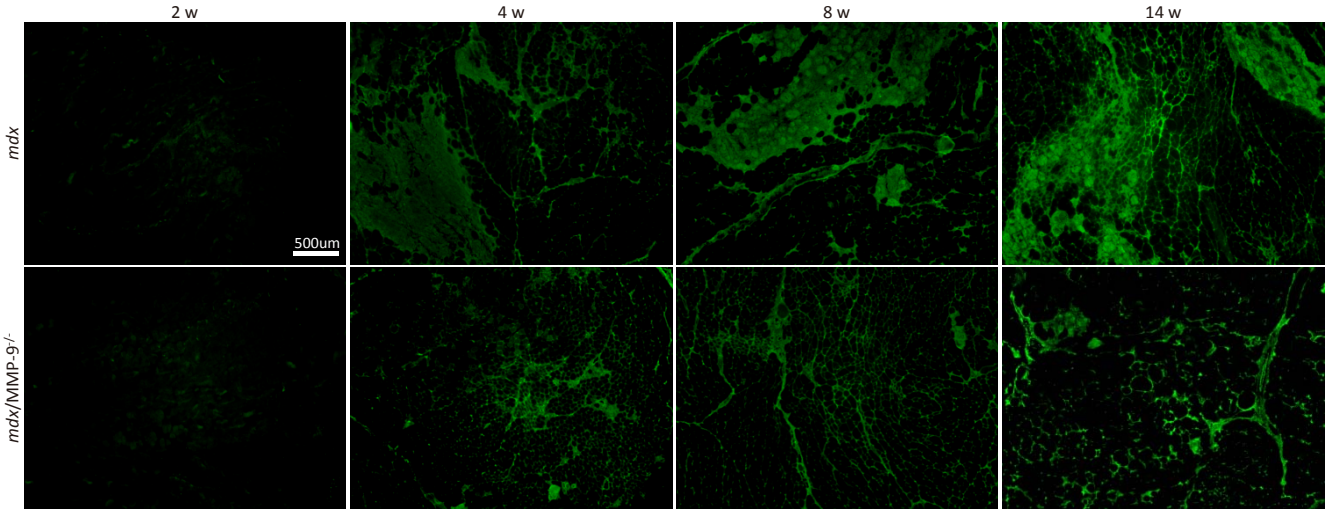

Fig. S4. MMP-9 ablation reduces muscle necrosis at the early disease stage in *mdx* mice.
TA muscle cryosections from *mdx* and *mdx*/*Mmp9*$^{-/-}$ mice, immunostained with Alexa Fluor 488-labeled anti-mouse immunoglobulin G (IgG) antibody to detect necrotic fibers at 2, 4, 8, and 14 weeks of age. Scale bar: 500 μm.

Fig. S5

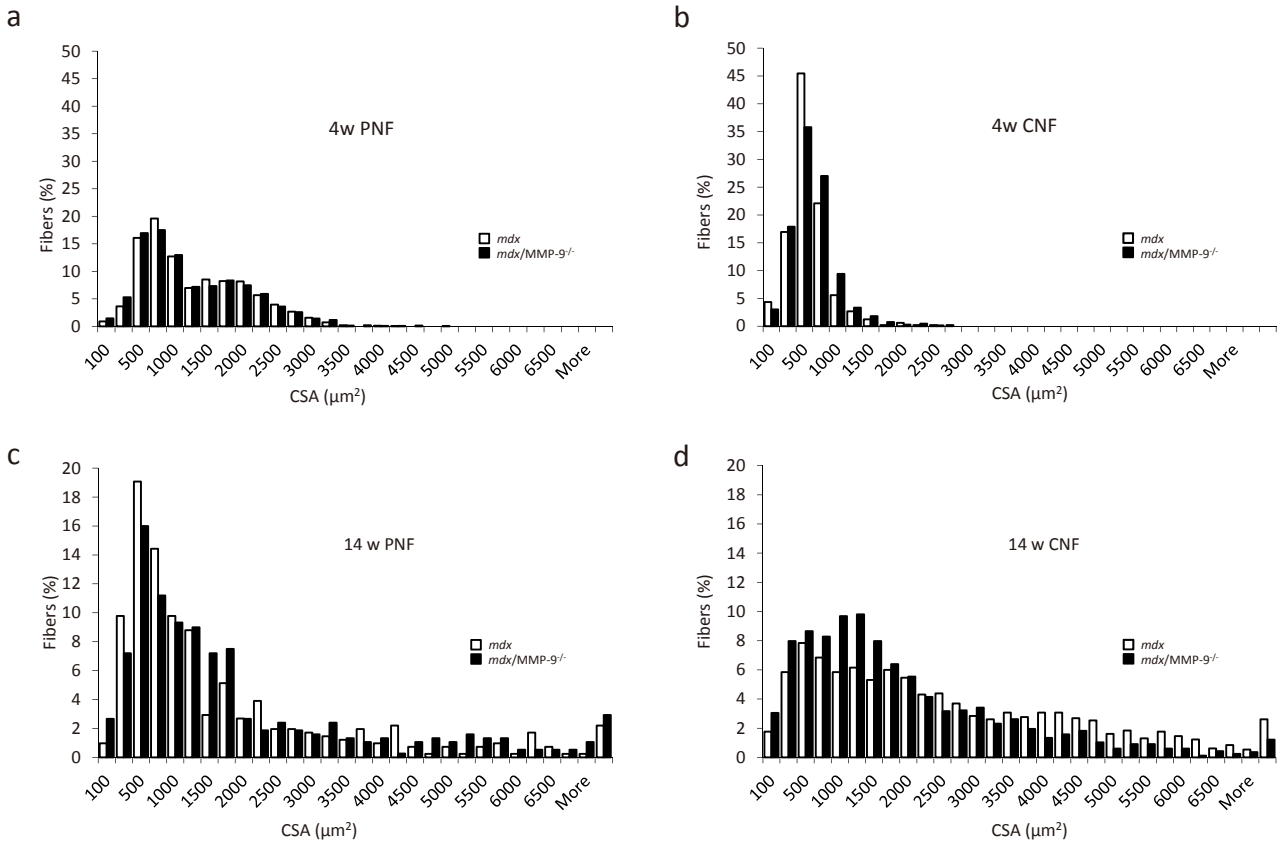

Fig. S5. MMP-9 ablation deteriorates the growth of regenerated fibers at 14 weeks of age in *mdx* mice.
a, b) Fiber size distribution of PNFs (a) and CNFs (b) in TA muscles of *mdx* and *mdx*/*Mmp9*$^{-/-}$ mice at 4 weeks of age. c, d) Fiber size distribution of PNFs (c) and CNFs (d) in TA muscles of *mdx* and *mdx*/*Mmp9*$^{-/-}$ mice at 14 weeks of age. (n = 3 per group). PNF: perinuclear fiber, CNF: centronuclear fiber.

Fig. S6

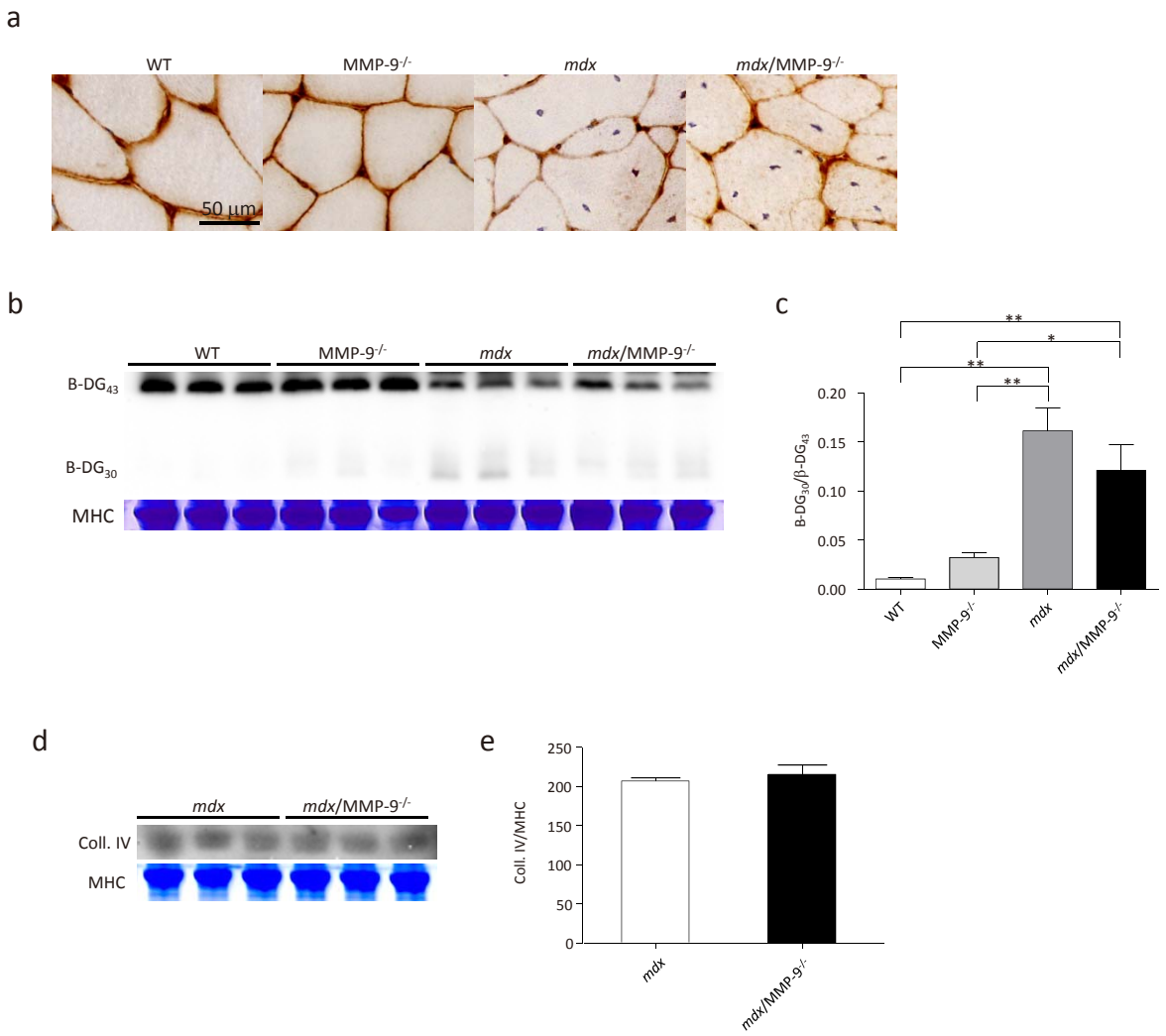

Fig. S6. MMP-9 ablation does not affect the β-DG and type IV collagen levels in the sarcolemma of *mdx* mice. a) Immunohistochemical staining of β-DG in TA muscles of WT, *Mmp9*$^{-/-}$, *mdx*, and *mdx*/*Mmp9*$^{-/-}$ mice at 8 weeks of age. Nuclei were counterstained with hematoxylin. Scale bar: 50 µm. b, c) Western blot probed for full-length β-DG (β-DG$_{43}$, upper bands) and cleaved 30 kDa proteins (β-DG$_{30}$, lower bands) in TA muscles of *mdx* and *mdx*/*Mmp9*$^{-/-}$ mice at 8 weeks of age (b). Relative protein levels of β-DG$_{30}$ to β-DG$_{43}$ shown in b) (c). d, e) Western blot probed for type IV collagen in TA muscles in *mdx* and *mdx*/*Mmp9*$^{-/-}$ mice at 8 weeks of age (d). Relative (to MHC) protein level of collagen type IV shown in d) (e). Data are presented as mean ± SEM (n = 3 per group). * $P < 0.05$, ** $P < 0.01$.

Fig. S7

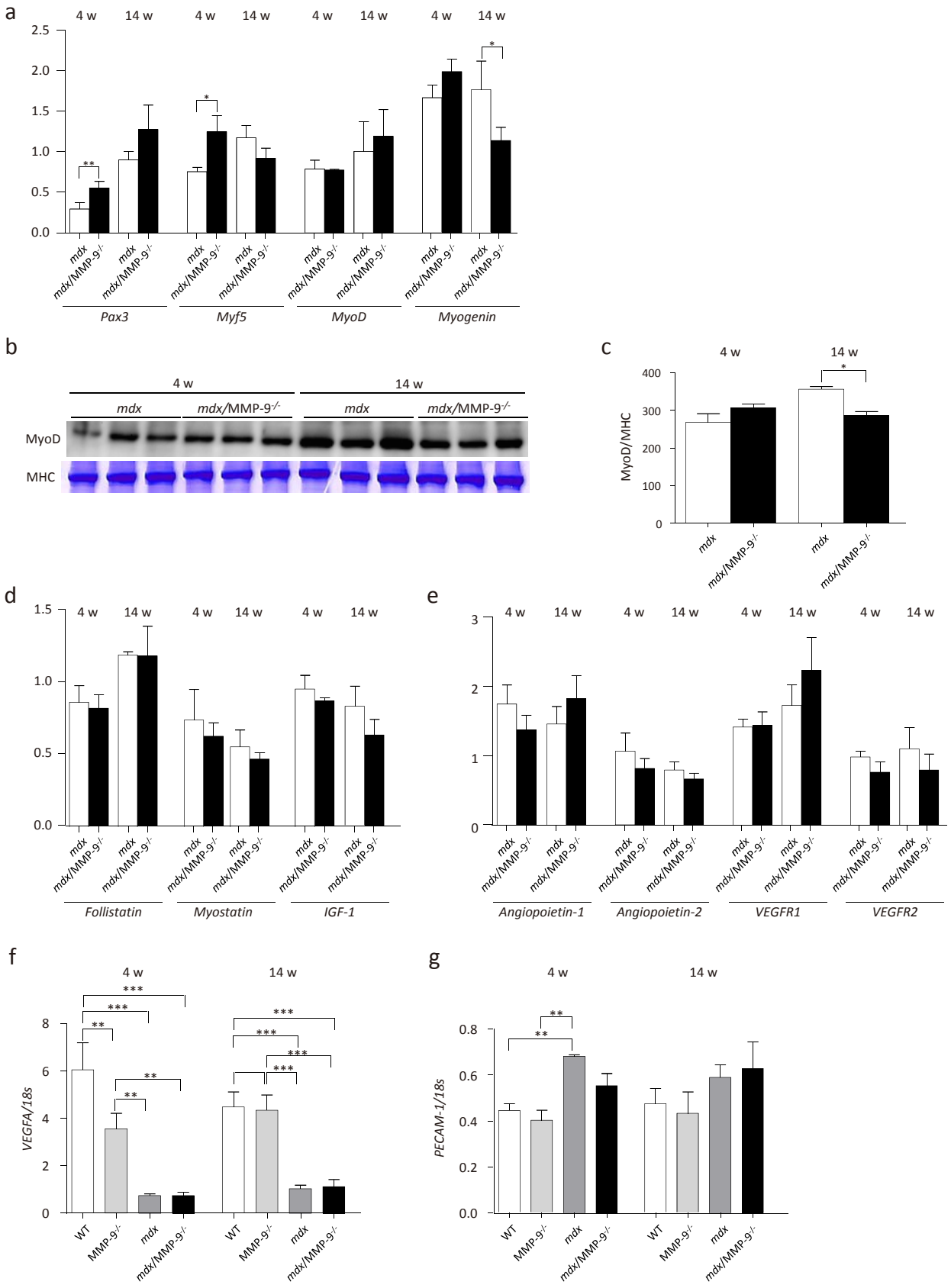

Fig. S7. Effects of MMP-9 ablation on expression of myogenic and growth factors in dystrophic muscle.

a) Relative (to *18S rRNA*) mRNA levels of myogenic transcripts *Pax3*, *Myf5*, *MyoD*, and *myogenin* in the gastrocnemius muscles of *mdx* and *mdx*/*Mmp9*$^{-/-}$ mice at 4 and 14 weeks of age. b, c) Western blot probed for MyoD in the gastrocnemius muscles of *mdx* and *mdx*/*Mmp9*$^{-/-}$ mice at 4 and 14 weeks of age. Relative (to MHC) protein levels of MyoD shown in b) (c). d, e) Relative (to *18S rRNA*) mRNA level of growth factors *follistatin*, *myostatin*, and *IGF-1* (d) and angiogenic factors *angiopoietin-1*, *angiopoietin-2*, *VEGFR*1, and *VEGFR2* (e) in the gastrocnemius muscles of *mdx* and *mdx*/*Mmp9*$^{-/-}$ mice at 4 and 14 weeks of age. F, g) Relative (to *18S rRNA*) mRNA level of *VEGFA* (f) and *pecam-1* (g) in the gastrocnemius muscles of WT, *Mmp9*$^{-/-}$, *mdx*, and *mdx*/*Mmp9*$^{-/-}$ mice at 4 and 14 weeks of age. Data are presented as mean $\pm$ SEM (n = 3 per group). * $P < 0.05$, ** $P < 0.01$, *** $P < 0.005$.